3.1 Ga 左右全球岩浆事件和地壳演化

边天一[1)],孟凡超[1,2,3)],杨飞[1)]

1）深层油气全国重点实验室[中国石油大学(华东)],山东青岛,266580;
2）青岛海洋科技中心海洋矿产资源评价与探测技术功能实验室,山东青岛,266237;
3）崂山国家实验室,山东青岛,266061

内容提要：全球克拉通 90%的陆壳可能是在太古宙形成,集中在 3.5~3.1Ga、2.8~2.7Ga、2.6~2.5Ga 三个阶段,2.8~2.7Ga 和晚期 2.6~2.5Ga 时期的岩石保留较多,地壳增生与改造机制研究较多,受样品稀少限制,3.0 Ga 之前的岩浆事件与陆壳形成演化研究相对薄弱,早前寒武纪岩浆事件与地壳增生方式仍存在争议。本文系统总结了全球中太古代(主要为 3.2~3.0Ga 期间)岩石的锆石年龄、岩石类型、全岩地球化学和锆石 Lu—Hf—O 同位素特征。主要认识包括:① 3.2~3.0Ga 时期岩石在全球各大洲均有分布,现今主要集中在北半球,而南半球的数量相对较少;② 岩石的锆石年龄峰值集中在约 3.05Ga 和约 3.15Ga 两个时期;③ 岩石的主要岩性为英云闪长岩和奥长花岗岩,具有过铝质的特征,不同地区呈现出不同的岩石组合,展现出一定的地区独特性;④ 不同地区岩石锆石的 $\varepsilon_{Hf}(t)$ 值表现出明显差异,反映了岩石起源和演化历史的差异性。大部分锆石的 $\delta^{18}O$ 值与地幔熔体处于平衡状态,也有部分锆石的 $\delta^{18}O$ 值较高,可达+8.93‰,暗示岩石源区经历了一定的低温蚀变或地壳物质的混染;⑤ 岩石呈现轻稀土元素富集、重稀土元素亏损的右倾模式,铕元素异常明显。整体上 Th、U、K、Pb 等元素相对富集,而 Nb、Ta、P、Sm、Ti 等元素相对亏损。综合研究表明:① 3.1Ga 左右 TTG 岩石可能由经历低温蚀变的玄武质岩石部分熔融形成。Hf 同位素特征显示,该时期玄武质岩石多数为 3.3Ga 左右时期由轻度亏损的地幔部分熔融形成。② 中太古代早期(主要为 3.2~3.0Ga 期间)发生了一次全球性质的岩浆活动和地壳增长事件,峰值期在约 3.05Ga 和约 3.15Ga。(3)类似于现代板块运动的构造体制在中太古代已经启动。

关键词:中太古代;地壳增生;岩浆事件;TTG 岩石

大陆地壳生长和演化研究是了解地球早期发展历史的关键,对认识古老克拉通的形成与地球环境演变具有重要意义(Zhai Mingguo and Santosh, 2011;Nance et al., 2014)。目前,早前寒武纪的陆壳形成、增生时间及机制仍存在争议。一种观点认为现今的地壳形成于地球演化的早期(>4.0Ga),其后新生地壳量等于或小于由于循环进入地幔的消耗地壳量,导致地壳累积增长曲线呈稳态变化或呈下降趋势(Armstrong, 1991;Sylvester et al., 1997)。另一种观点认为地壳在整个地质历史时期一直处于增长状态,太古宙早期,地壳增长速度较快,以后渐慢,地壳增长一直以稳定的速度进行(Taylor and Mclennan, 1995)。无论哪种模式,都认为太古宙是地壳增长的重要时期,而新元古代到显生宙,地壳增长量十分有限。

近年来,古老克拉通大量的同位素年龄数据表明,克拉通 90%的陆壳可能是在早前寒武纪形成,其主要形成期集中在 3.5~3.1 Ga、2.8~2.7 Ga、2.6~2.5 Ga 三个阶段(Hawkesworth and Kemp, 2006;Condie and Aster, 2010;Zhai Mingguo and Santosh, 2011)。其中,新太古代早期(2.8~2.7 Ga)和晚期(2.6~2.5 Ga)被认为是全球克拉通大陆地壳巨量生长最为关键的时期(Khanna et al., 2014;Hayman et al., 2015;Tang Ming et al., 2020),受样品稀少的限制,3.5~3.1 Ga 时期陆壳形成演化的研究相对薄弱。Shirey 等通过对澳大利亚卡普瓦尔、西伯利亚、加拿大 Slave 克拉通和津巴布韦等五个古老克拉通产出的钻石进行研究发现,钻石中包裹体内的

注:本文为国家自然科学基金资助项目(编号:42272225)、崂山实验室科技创新项目(编号:LSKJ202203401)、山东省自然科学基金面上项目(编号:ZR2021MD083)和中央高校基本科研业务费专项(编号:23CX09004A)的成果。
收稿日期:2024-10-21;改回日期:2024-12-09;网络首发:2024-12-20;责任编辑:章雨旭。Doi: 10.16509/j.georeview.2024.12.065
作者简介:边天一,男,2000 年生,硕士研究生,地质学专业;Email: 1390485955@qq.com。通讯作者:孟凡超,男,1982 年生,博士,教授,主要从事岩石学及地球化学教学与科研;Email: mengfc@upc.edu.cn。

物质在 3.2~3.0 Ga 期间发生了较大转变,之前为以橄榄岩为主,之后是以榴辉岩为主(Shirey and Richardson, 2011)。另外,TTG 岩石(tonalite—trondhjemite—granodiorite,即英云闪长岩—奥长花岗岩—花岗闪长岩,构成的岩石组合)的 Rb/Sr、K_2O/Na_2O、Sr/Y 和$(La/Yb)_N$比值和玄武岩、科马提岩等基性岩的 Ba/La、Ba/Nb、U/Nb 和 Pb/Nd 比值,在约 3.15 Ga 前后都发生了显著变化(Shirey and Richardson, 2011;邓晋福等,2015;张旗等,2024;张金朋等,2024)。这些变化都说明,3.2~3.0Ga 可能是地球地壳形成演化的一个关键转折阶段。甚至,有些学者认为板块构造运动就可能起始于 3.2~3.0 Ga 期间(Dhuime et al., 2012, 2015;吴鸣谦等,2014;Gamal El Dien et al., 2020;Windley et al., 2021)。

受古老地壳岩石样品稀少的限制,前人对 3.2~3.0 Ga 时期岩石的成因及地壳形成演化的研究多集中于地球化学数值模拟(Windley et al., 2021)。对实际地质样品的研究相对较少,仅有的几个克拉通古老岩石的研究也比较独立,缺少全球性的对比。本文对全球 3.1 Ga 左右岩石和锆石的地质记录进行系统梳理,总结了其锆石年龄分布、地球化学、Lu—Hf—O 同位素组成特征,系统对比了全球主要克拉通 3.1 Ga 左右岩石的时空分布、物质组成、地球化学以及同位素特征,探讨中太古代岩石成因为早期地壳生长与演化提供关键信息。

1 3.1 Ga 左右岩石和锆石的时空分布特征

统计表明,全球约 10 余个克拉通中保存有 3.1 Ga 左右时期的岩石,22 个克拉通见有 3.1 Ga 左右时期的岩浆锆石和碎屑锆石(附表,纸质印刷本略,见网络版:www.geojournals.cn/georev;图 1),主要特征如下:

(1)在现今构造格局下,岩石主要分布在北半球地区,南半球仅在东南极地盾区和澳大利亚部分

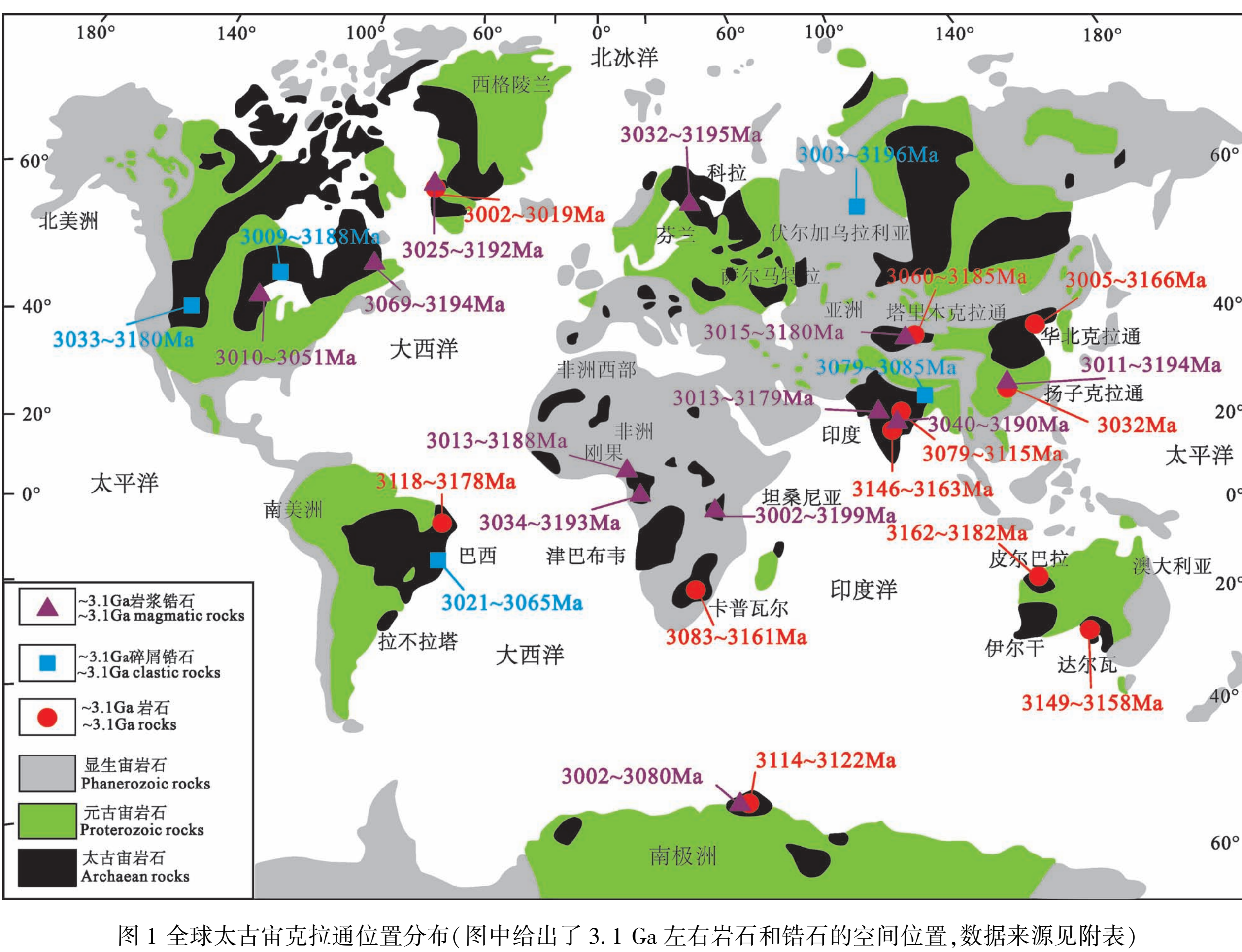

图 1 全球太古宙克拉通位置分布(图中给出了 3.1 Ga 左右岩石和锆石的空间位置,数据来源见附表)

Fig. 1 Distributions of global Archeancratons(showing spatial distribution of ~3.1 Ga rocks and zircons)(modified from Tang Yanjie et al., 2013. See attached table for data details)

地区有发现,出露范围很小,多以脉体形式穿插于其他岩石之中;锆石分布广泛,遍布全球,北半球明显多于南半球。在发现的约 3.1 Ga 锆石中,碎屑锆石与岩浆锆石数量相当,但在非洲刚果、津巴布韦克拉通和印度部分地区岩浆锆石数量明显多于碎屑锆石。其在 3.1 Ga 左右时分布特征还需进一步研究(张世红灯,2002;张拴宏等,2022)。

(2)岩石以 TTG 岩石为主,少量闪长岩、辉长岩等岩石,在欧洲一处蛇纹岩中也存在 3.1 Ga 左右岩石。

(3)并非所有 3.1 Ga 左右 TTG 岩石都伴随有表壳岩存在,仅在华北克拉通、圣弗朗西斯科克拉通、乌克兰地盾、印度库克地块、达尔瓦克拉通、西格陵兰 6 个地区发现有表壳岩,它们具有相似的岩石组合,由变质泥岩、变质砾岩和 BIF 组成。

(4)岩石普遍遭受后期变质作用改造形成片麻岩,原始岩石几乎不可分辨。

(5)3.1Ga 左右的碎屑锆石多发现于太古宙岩石中(3.0~2.5 Ga),也有少量出现在元古宙和现代河流沉积物中。

从全球约 3.1 Ga 锆石和岩石年龄统计(图 2 和图 3),可以看出:① 3.1 Ga 左右岩石存在三个明显的年龄峰值,分别为 3.0 Ga、3.05 Ga 和 3.15 Ga。② 锆石年龄存在两个明显的年龄峰,分别为 3.0 Ga 和 3.15 Ga。③ 各克拉通约 3.1 Ga 锆石年龄均存在相似的 3.15 Ga 峰值(南美洲亚马逊和圣弗朗西斯科克拉通除外)。说明约 3.15 Ga 时期的岩浆事件具有全球性,而 3.0 Ga 和 3.05 Ga 两次岩浆事件仅在局部发生,不具备全球性。

1.1　亚洲地区

华北克拉通是欧亚大陆东部最大的克拉通之一,已在 5 个地区发现 3.1 Ga 岩石,但规模都很小。鞍山—本溪地区,3.1 Ga 岩石以包体或侵入体的形式与更古老岩石一同构成白家坟、东山、深沟寺和锅底山杂岩(万渝生等,2001;周红英等,2007,2008;Wu Fuyuan et al., 2008;Wan Yusheng et al., 2012;董春艳等,2013)。冀东,黄柏峪和曹庄,喇叭山岩系变质碎屑沉积岩中存在 3.1 Ga 左右岩石和碎屑锆石。最近,Meng(2022)等在渤海湾盆地钻孔岩芯样品中发现 3.1 Ga 左右岩石,说明渤海湾盆地存在中太古界基底(孙会一等,2016;万渝生等,2021;Meng Fanchao et al., 2022)。鲁西地区,新太古代早期岩石中存在大量 3.1 Ga 左右锆石颗粒,认为该区可能存在一个中太古代陆核(Gao Lei et al., 2019;Yu Yang et al., 2022)。辽北地区,3.1 Ga 左右的岩石主要分布在栾家界地区(Li Dapeng et al., 2020;Liu Jin et al., 2022)。

扬子克拉通 3.1 Ga 左右岩石分布于南部的崆岭杂岩和撮科杂岩。最近,在崆岭杂岩中获得片麻岩岩石年龄为约 3.0 Ga,并获得 3.1 Ga 的两阶段 Hf 模式年龄(Qiu Xiaofei et al., 2018a;Qiu Xiaofei et al., 2018b;邱啸飞等,2022)撮科杂岩中也发现 3.11~3.06 Ga 太古宙基底岩石,这些岩石由古太古代至中太古代早期的新生地壳物质改造形成(Zhang

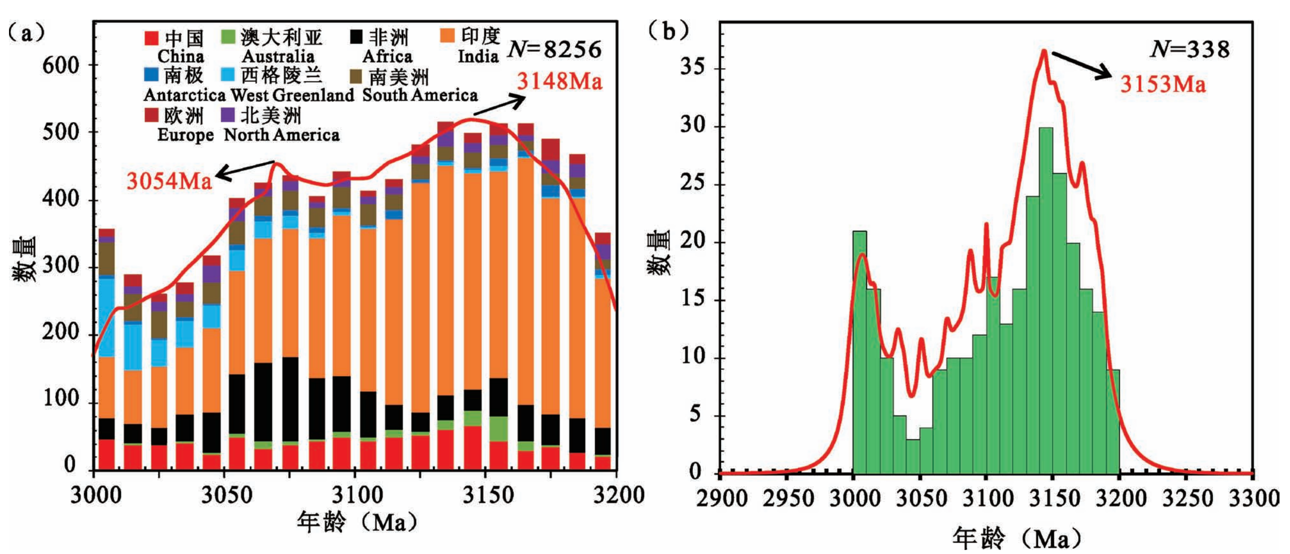

图 2 (a)全球~3.1 Ga 锆石年龄分布图(数据详情见附表);(b)全球~3.1 Ga 岩石年龄分布图(数据详情见附表)

Fig. 2 (a) Global ~3.1 Ga zircons age distribution (see attached table for data details); (b) Global ~3.1Ga rocks age distribution (see attached table for data details)

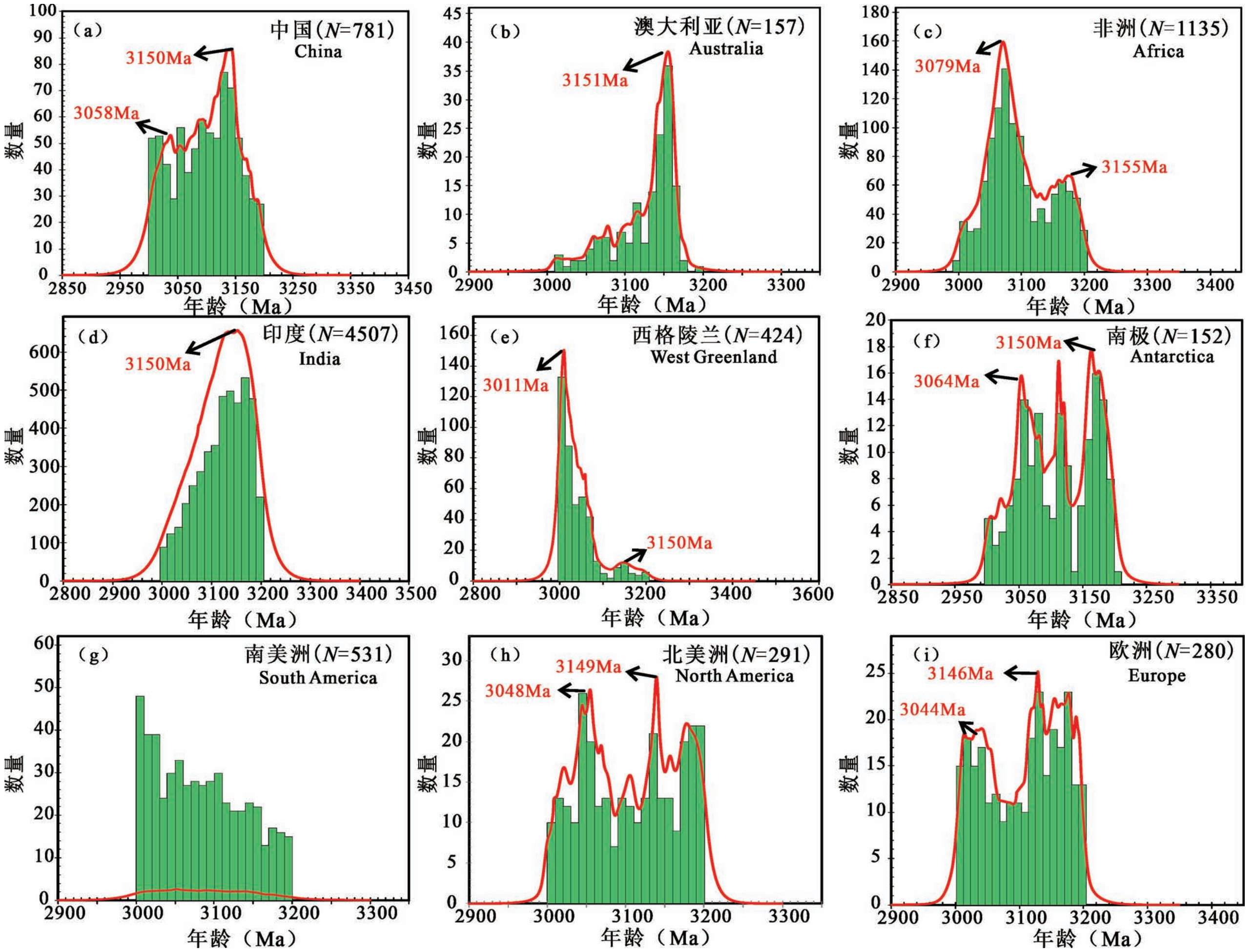

图 3 全球各地区 3.1Ga 左右岩石年龄分布直方图

Fig. 3 Histograms of age distribution from ~3.1Ga rocks

Shaobing et al., 2006; Cui Xiaozhuang et al., 2018)。

塔里木克拉通边缘地区广泛分布着太古宙露头岩石。塔里木盆地西南缘赫罗斯坦岩群中发现紫苏辉石麻粒岩,其锆石 U-Pb 年龄为 3137±4 Ma,是塔里木克拉通存在中太古代古老陆核和大规模地壳生长的直接证据(Zhang Chuanlin et al., 2013;郭新成等,2013;Ge Rongfeng et al., 2013;Ge Rongfeng et al., 2022)。敦煌东巴兔山干沟地区片麻岩中,从 45 颗锆石中获得约 3.06 Ga U-Pb 表面年龄,是目前为止敦煌最古老的岩石,对指示敦煌地区的构造归属具有重要意义(赵燕等,2015)。

印度太古宙克拉通广泛分布于中—南部地区。达瓦克拉通西部以 3.1~3.0 Ga 岩浆岩为主,$\varepsilon_{Hf}(t)$ 值为负值,暗示这些岩石是由古老地壳重熔而来(Maibam et al., 2016; Ao Wenhao et al., 2021)。Sargur 群代表达瓦克拉通较老绿岩带,由以超镁铁质玄武岩为主的火山序列与层间变质沉积物组成,其锆石表面年龄为 3200~3106Ma(Jayananda et al., 2015;Guitreau et al., 2017;Dasgupta et al., 2019;Ravindran et al., 2023)。Arsikere,Bellur 和霍纳加纳哈利(Honaganahalli)地区的正片麻岩,二长花岗岩和花岗片麻岩等岩石均获得了 3.1~3.0 Ga 锆石年龄(Maibam et al., 2011;Jayananda et al., 2019;Ao Wenhao et al., 2021)。辛格布姆克拉通 3.1 Ga 左右岩石分布于辛格布姆花岗杂岩和古铁矿群。其中辛格布姆花岗杂岩的侵位一直持续到中太古代(3120 Ma 和 3050 Ma)(Misra, 2006),马尤布汉杰(Mayurbhanj)花岗岩套中获得了一致的锆石结晶年龄(3080±8 Ma,3092±5 Ma(Mishra et al., 1999);3084±3 Ma(Nelson et al., 2014);3063±11 Ma(Upadhyay et al., 2019)。古铁矿群中博奈花岗岩套具有较年轻的锆石结晶年龄(3.16 Ga),与辛格

布姆花岗杂岩在年龄上相当。另外,在苏金达—瑙萨希地区发现一套锆石 U-Pb 年龄为 3123±7 Ma 和 3119±6 Ma 的层状铁镁质—超铁镁质侵入体(Monda et al., 2006;Khatun et al., 2014)。巴斯塔尔克拉通 3.1 Ga 左右岩石分布于苏克马(Sukma)群中,其最大沉积年龄为 3128±6 Ma(Nandi et al., 2023)。除此之外,印度南部库尔格(Coorg)地块、阿拉瓦利和本德尔坎德克拉通也发现了 3.1 Ga 左右铁镁质—超铁镁质岩石和 TTG 岩石(3189±5 Ma)(Santosh et al., 2016;Amaldev et al., 2016;Yang Qiongyan et al., 2016;Yu Bing et al., 2021;Yang Chengxue et al., 2023;Kaur et al.,2021,2022)。

西伯利亚(Siberian)克拉通位于俄罗斯东部,是亚洲最大的前寒武纪克拉通。目前,仅在阿纳巴尔(Anabar)地区发现有 3.12 Ga 左右石榴子石云母片麻岩、约 3.19 Ga 石榴子石麻粒岩和 3.1 Ga 左右碎屑锆石(Rosen et al., 2006;Paquette et al., 2017;Shatsky et al., 2022)。这些证据证实西伯利亚克拉通存在 3.1 Ga 左右时期太古代地壳生长事件。

1.2 大洋洲

澳大利亚西部和南部地区太古宙克拉通分布广泛,包括皮尔巴拉(Pilbara)克拉通、高勒(Gawler)克拉通和伊尔冈(Yilgarn)克拉通。皮尔巴拉克拉通古陆核可以分为东、西皮尔巴拉地体两部分。在东皮尔巴拉地体的英云闪长岩和火山沉积岩中获得 3.1 Ga 左右锆石年龄(Kranendonk et al., 2010)。西皮尔巴拉地体相对年轻,已在 3 个地区发现 3.1 Ga 左右岩石,包括邵尔地体火山碎屑岩与花岗片麻岩(3.13~3.11 Ga)(Smithies et al., 2005)、谢拉塔杂岩东部的黑云母英云闪长岩(3.07 Ga)和克里夫维尔组长英质凝灰岩中的继承锆石(3.195 Ga)(Kranendonk et al., 2007)。高勒克拉通新发现了约 3.15 Ga 中太古代岩石,出露范围较广,把克拉通构造演化历史向前推进 500 Ma 左右(Fraser et al., 2010)。伊尔冈克拉通克拉通被划分为 5 个主要部分,已在 4 个地体中获的 3.1 Ga 左右岩石,包括默奇森东部地体(3.17 Ga)、南十字星花岗岩—绿岩带(3.05Ga)、纳瑞尔地体石英岩(3.1 Ga)和西南地体石英岩(3.177 Ga、3.05 Ga)(Kinny et al., 1990;Bosch et al., 1996;Chen Shefa et al., 2003)。

1.3 非洲

非洲太古宙克拉通分布于中部和南部地区。卡普瓦尔(Kaapvaal)克拉通中东部于 3.1 Ga 左右进行第一次克拉通化,该地区 3.1 Ga 左右花岗岩面积超过 20000 km^2(Belcher et al., 2006)。在斯威士兰中部存在大规模沉积记录(3.16 Ga)和麻粒岩相变质记录(3.11~3.07 Ga),这些记录被解释为增生边缘沉积(Taylor et al., 2012,2019)。斯威士兰西部存在大型花岗岩基岩,从中获得 3.15~3.08 Ga 锆石 U-Pb 年龄和 3.11 Ga 全岩 Sr—Nd 等时线年龄。(Moser et al., 2001;Westraat et al., 2005;Suhr et al., 2014)。刚果(Congo)克拉通 3.1 Ga 左右岩石分布于克拉通西北部 Ntem 杂岩中,包括沉积变质岩(3.14~3.07 Ga)、辉石花岗岩套和 TTG 岩套(3.15 Ga),其中 TTG 岩套被解释为在俯冲—增生构造模式下形成(Akame et al., 2020)。在马达加斯加 Antongil 克拉通南部变质沉积物中,获得了 3178 Ma 变质流纹岩和 3187 Ma 黑云母片麻岩,可能当时存在一个中太古代陆核。

1.4 北美洲

格陵兰岛南部基亚地体研究历史较长。早期研究认为,基亚地体是由 3076~3068Ma 岩浆弧形成,存在拉斑玄武岩和钙碱性安山岩(Garde, 2007;Szilas et al., 2015,2017)。诺兰特(Nordlandet)杂岩是基亚地体最古老的部分,由约 3.19 Ga 闪长片麻岩组成,受到 3.05 Ga 英云闪长岩侵入影响。在菲斯克峡湾(Fiskefjord)杂岩和阿兰瓜杂岩中获得了约 3180 Ma 变质闪长岩和小型捕虏体、3134~3131 Ma 麻粒岩以及大量 3015 Ma 深成侵入岩。具有相似锆石年龄的片麻岩在菲斯克峡湾杂岩内部和周围也普遍存在(Nutman et al., 2004;Kirkland et al., 2018;Kirkland et al., 2020;Steenfelt et al., 2020;Yakymchuk et al., 2020;Waterton et al., 2020;Olierook et al., 2021)。基亚地体北部是未分化的麻粒岩和角闪岩相正片麻岩,它们含有基性上地壳岩石的残余。岩石组合类型与菲斯克峡湾杂岩相似,但年龄相对较小,约 3020Ma(Scherstén et al., 2013;Gardiner et al., 2019)。并发育小型碳酸盐岩侵入体(3007±2Ma)(Bizzarro et al., 2002)。

苏必利尔(Superior)克拉通是北美古地核重要组成部分,3.1 Ga 左右岩石分布于克拉通西北部萧提(Solit)湖块体、东盟(Assean)湖块体和皮尔森(Pearson)湖块体,前人研究认为萧提湖块体、东盟湖块体具有相同的 3.16~3.2Ga 中太古代深成作用事件(Böhm et al., 2003)。其余地区零星分布着~3.1Ga 太古宙岩石,如北加勒比海地区(3122±13 Ma)、温尼伯河(Winnipeg)地区(3111±14 Ma)、英(English)河地区(3069±14 Ma、3122±13 Ma)、坦尼

斯湖地区(3055±4 Ma、3150 Ma)、明尼苏达河地区(3140 Ma)等,这些地体所记录的中太古代事件与花岗岩—绿岩地体的初始形成有关(Melnyk et al., 2006;Bickford et al., 2006;Lankvelt et al., 2016;Li Dengfeng et al., 2020;Strong et al., 2022)。

怀俄明克拉通中部的巴洛峡(Barlow Gap)群基底石英岩中含有 3.2~3.1Ga 碎屑锆石(Grace et al., 2006)。蒙大拿州西南部、北部和萨卡维(Sacawee)地块中,3.1 Ga 左右高铝奥长花岗岩和长英质岩石侵入古太古代麻粒岩中(Gifford et al., 2014)。明尼苏达(Minnesota)州西南部的蒙得维亚(Montevideo)省和莫顿(Morton)地区发现了复杂的 3.1 Ga 左右岩石,岩性为花岗闪长混合岩、花岗片麻岩和花岗闪长岩侵入体(3140±5Ma),锆石外围存在 3.2~3.0 Ga 生长痕迹,说明该地区 3.1 Ga 左右发生剧烈岩浆活动导致古老岩石变质和新地壳的生长(Schmitz et al., 2006)。

1.5 南美洲

圣弗朗西斯科(São Francisco)克拉通由太古宙花岗片麻岩组成。克拉通北部 3.1 Ga 左右岩石主要分布于加维昂(Gavião)地块和塞里尼亚(Serrinha)地块,包括 TTG 片麻岩(3180~3000 Ma)(Peucat et al., 2002;Oliverira et al., 2020;Barbosa et al., 2020)和混合岩(3.08~2.98 Ga)(Oliverira et al., 2010)。乌阿(Uauá)地块与塞里尼亚地块接壤,其最古老岩石为 3.15~3.12 Ga 条带状片麻岩。此外,该区还发现了 3.13~3.12Ga 英云闪长岩和 3.13~3.07 Ga 长英质火山岩(Oliverira et al., 2010,2019)。安布罗休(Ambrósio)地块中混合岩包体,其锆石结晶年龄为 3.1 Ga(Mello et al., 2006)。

拉普拉塔克拉通尼科皮雷斯(Nico PeÂrez)地体中心有两个太古宙单元, La China 杂岩和山雀(Las Tetas)杂岩。前人在此处发现了 3096 Ma 岩石和 3.12~3.16 Ga 的锆石(Gaucher et al., 2011;Masquelin et al., 2021)。

在巴西东北部博尔博雷玛(Borborema)省存在南美洲最古老的地壳碎片:São José do Campestre 地块。该地块两侧存在约 3.18 Ga 奥长花岗质片麻岩,并被约 3.0 Ga 辉长斜长岩侵入(Dantas et al., 2004)。在巴西西部亚马逊(Amazonian)克拉通中发现有两个太古宙陆核(Juliani et al., 2010;Fernandes et al., 2021):卡拉加斯(Carajas)是一个典型花岗岩—绿岩地体,包含约 3.04 ~ 2.99 Ga 绿岩带和花岗岩类(Almeida et al., 2011,2013);而卡拉吉(Caraj)存在太古宙岩石,包括约 3.06 Ga TTG 片麻岩和混合岩、约 3.0 Ga 麻粒岩和约 3.0 Ga 钙碱性英云闪长岩(Moreto et al., 2011,2015a,2015b)。

1.6 欧洲

萨尔玛提亚(Sarmatia)克拉通是东欧地台基底南部部分,由沃罗涅日结晶地块和乌克兰地盾组成。在沃罗涅日结晶地块,3.1 Ga 左右岩石包括科马提岩—拉班玄武岩(3.2~3.0 Ga)(Chernyshov et al., 2014)和谢尔盖耶夫(Sergiev)橄榄杂岩中的蛇纹岩(3136 Ma)(Lobach-Zhuchenko et al., 2017)。在乌克兰地盾,中第聂伯省绿岩带的形成可分为两个阶段:3.19~3.14 Ga 火山系列岩石和 3.07 Ga 铁镁质熔岩(Sukach et al., 2014)。同时期还形成萨尔蒂科夫卡(Saltykovka)杂岩(3029 Ma 和 3091 Ma)(Lobach-Zhuchenko et al., 2017)和位于亚速省(Azov province)中部、北部和西部的绿岩带(3095Ma 和 3157Ma)。

芬诺斯堪迪亚(Fennoscandian)地盾在三个地区发现了 3.1 Ga 左右 TTG 片麻岩:①芬兰北部元古代岩石中一个小穹隆的奥长花岗质片麻岩,其锆石 U-Pb 和 Sm-Nd 全岩年龄均为 3.1Ga(Kröner et al., 1981,1990);②芬兰中部卡累利阿克拉通最西端的伊萨尔米(Lisalmi)杂岩,由花岗闪长岩(3095±18 Ma)、石英闪长岩(3173±7 Ma)、混合角闪岩、麻粒岩和火成岩组成(Mänttäri et al., 2002;Lauri et al., 2011; Mikkola et al., 2011);③伏德洛泽罗(Vodlozero)省西北部存在英云闪长岩(3.2~3.1 Ga)和混合岩(Sergeev et al., 2007,2008)。

1.7 南极洲

3.1 Ga 左右岩石分布于南极洲面向印度洋扇区的 Denman 冰川地区、鲁克(Ruker)杂岩、恩德比地(Enderby Land)的纳皮尔(Napier)杂岩和 Mawson 海岸沿线。另外, 3.1 Ga 左右花岗质片麻岩、英云闪长岩、辉长岩等岩石分布于横贯南极山脉的 Nimrod 杂岩中(Sheraton et al., 1987;Grew et al., 1988;Boger et al., 2006,2008;Mikhalsky et al., 2006,2010)。

2 3.1 Ga 左右岩石的岩石类型与岩石学特征

全球超过 10 个克拉通中见有 3.1 Ga 左右岩石。约 50%为花岗岩,其中 30%为 TTG 岩石,以奥长花岗岩和英云闪长岩为主,花岗闪长岩很少出露;

约 15%为未被具体命名的片麻岩，其中格陵兰岛发现最多，其余分布在南极、美洲和非洲的部分克拉通；约 7%为变质沉积岩，包括变质泥岩和变质砾岩，主要分布在华北、达瓦、南非、圣弗朗西斯科等克拉通；约 10%为基性岩、超基性岩，根据前人文献所述，多为地幔物质直接侵入到地壳中；华北克拉通塔里木、印度库格地块等地发现有高级变质作用形成的麻粒岩，皮尔巴拉、库格地块和萨尔玛提亚等克拉通中发现的流纹岩和凝灰岩等火山喷发物质，是地壳生长最直接的证据。

3.1 Ga 左右岩石数据点在 An—Ab—Or 图中大多数落于英云闪长岩区与奥长花岗岩、花岗岩交界处（图 4a），结合前人报道的岩石岩性类型，说明 3.1 Ga 左右岩石以英云闪长岩和奥长花岗岩为主，数据显示 3.1 Ga 左右岩石岩性和分布十分复杂。华北克拉通鞍山地区和塔里木克拉通主要为奥长花岗岩，扬子克拉通主要为花岗岩；皮尔巴拉克拉通和西南格陵兰数据点落于英云闪长岩区域；花岗闪长质岩基本只位于西伯利亚克拉通和萨尔玛提亚克拉通，其他地区几乎没有花岗闪长岩区数据点；卡普瓦尔克拉通和刚果克拉通数据点主要在奥长花岗岩和花岗岩区，其他岩性区域几乎没有。3.1 Ga 左右岩石多为过铝质岩石（图 4b），只有极少数印度克拉通岩石位于准铝质区域。英云闪长岩和花岗闪长岩具

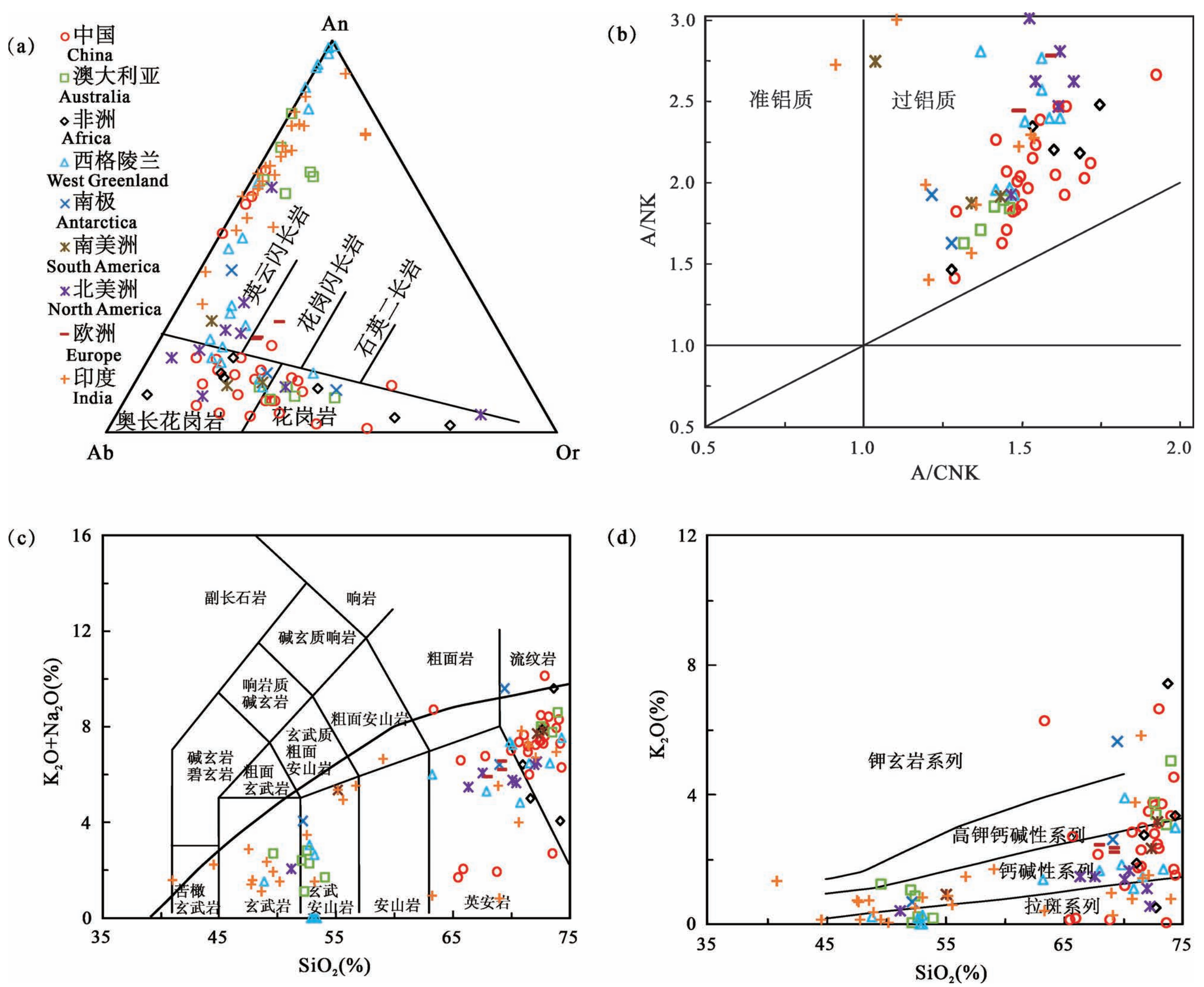

图 4 （a）全球约 3.1 GaTTG 岩石的 An—Ab—Or 图解（数据来源同图 2）；（b）全球约 3.1 GaTTG 岩石的 A/CNK—A/NK 图解（数据来源同图 2）；（c）全球约 3.1 GaTTG 岩石的 ATS 图解（数据来源同图 2），（d）全球约 3.1 GaTTG 岩石的 SiO_2—K_2O 图解（数据来源同图 2）

Fig. 4 (a) An—Ab—Or diagram of global ~3.1 Ga old TTG rocks (source of data same as Fig. 2); (b) A/CNK vs A/NK diagram of global ~3.1 Ga old TTG rocks (source of data same as Fig. 2); (c) ATS diagram of global ~3.1 Ga old TTG rocks (source of data same as Fig. 2), (d) SiO_2 vs K_2O diagram of global ~3.1 Ga old TTG rocks (source of data same as Fig. 2)

有较高 A/NK 值。岩石数据点普遍位于流纹岩区和英安岩等酸性岩区(图 4c)(邓晋福等,2015)。西南格陵兰、圣弗朗西斯科克拉通、亚马逊克拉通、苏必利尔克拉通、怀俄明克拉通和西伯利亚克拉通岩石属于钙碱性系列,少部分位于拉斑系列(图 4d);而皮尔巴拉克拉通和华北克拉通一部分岩石位于高钾钙碱性系列(图 4d)。

3 3.1 Ga 左右锆石的 Hf—O 同位素特征

本文收集了全球约 3.1 Ga 岩石主微量元素数据、锆石 Hf—O 同位素数据,选取不谐和度小于 15%的锆石^{207}Pb/^{206}Pb 表面年龄与相应锆石的 Hf 同位素进行分析。全球 3.1 Ga 左右 TTG 岩石的锆石 Hf 同位素具有以下特征:

(1)不同地区 $\varepsilon_{Hf}(t)$表现出明显差异,如辛格布姆克拉通、巴斯塔尔克拉通、华北克拉通、扬子克拉通、卡普瓦尔克拉通和皮尔巴拉克拉通、高勒克拉通 $\varepsilon_{Hf}(t)$值多为正值(-16.18~12.67),但位于亏损地幔线之下,说明这些地区岩石主要为新生地壳,同时伴随有强烈壳内再循环作用;而圣弗朗西斯科克拉通、拉普拉塔克拉通、亚马逊克拉通、苏必利尔克拉通、怀俄明克拉通、西伯利亚克拉通、萨尔玛提亚克拉通 $\varepsilon_{Hf}(t)$值多为负值(-12.3~5.96),说明这些地区约 3.1 Ga 岩石主要为壳内再循环产生,但有少量地幔物质添加。

(2)同一地区不同时代的锆石 Hf 同位素组成也呈现明显差异,如华北克拉通、达瓦克拉通、辛格

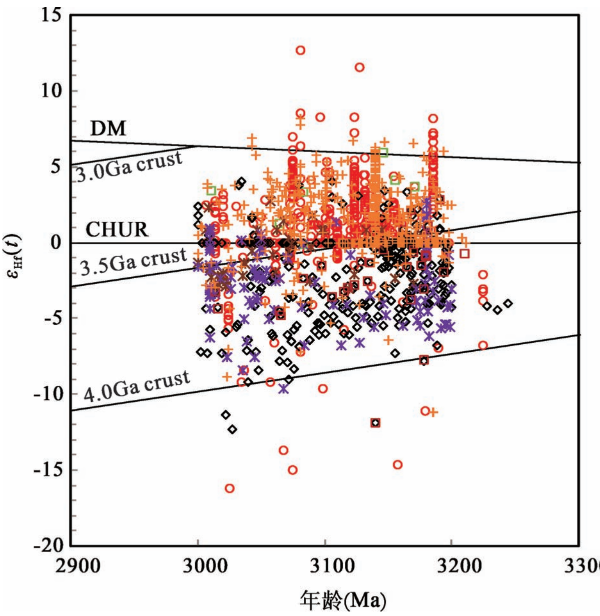

图 5 全球约 3.1 GaTTG 岩石锆石年龄-$\varepsilon_{Hf}(t)$图解(数据来源同图 2;图例同图 4)

Fig. 5 $\varepsilon_{Hf}(t)$ vs. Zircon age diagram for rocks from the world (source of data same as Fig. 2; figure legend same as Fig. 4)

布姆克拉通,随着年龄减小,$\varepsilon_{Hf}(t)$呈现下降趋势,同时负值的数据点明显增多,说明 3.1 Ga 左右早期,这些地区主要为新地壳的形成,到 3.0 Ga 左右时期则变为古老地壳的再循环。总体而言,随着时间的推移,地幔物质的添加减少,壳内再循环作用增加。

约 3.1 Ga 锆石的氧同位素具有类似该时期地

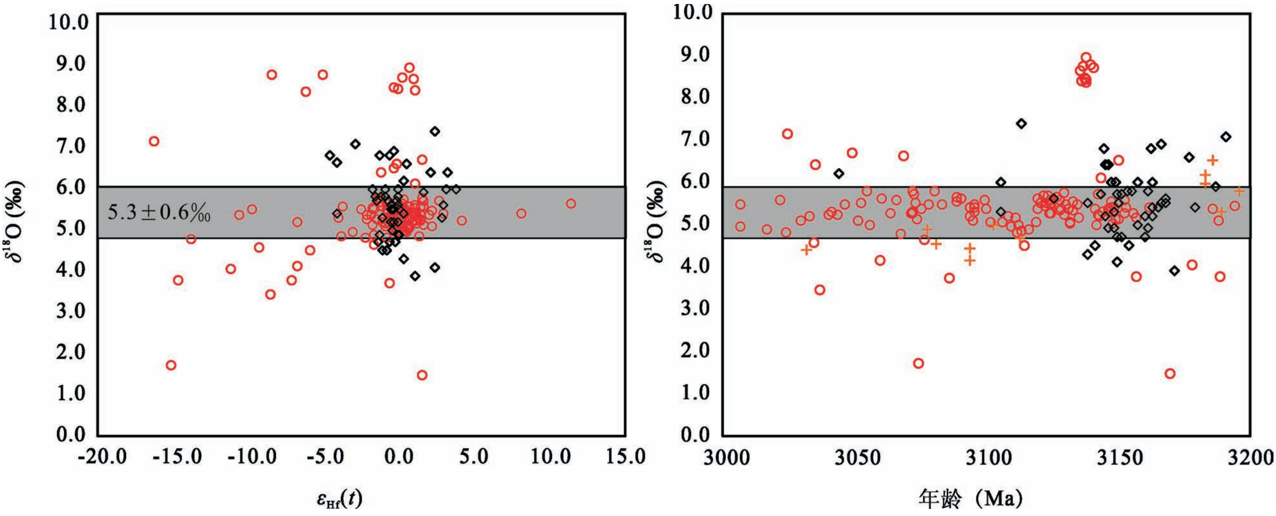

图 6 锆石 δ^{18}O 与 $\varepsilon_{Hf}(t)$、^{207}Pb/^{206}Pb 年龄的关系(数据来源同图 2;图例同图 4)

Fig. 6 Diagrams of $\varepsilon_{Hf}(t)$ and ^{207}Pb/^{206}Pb versus δ^{18}O (source of data same as Fig. 2; figure legend same as Fig. 4)

幔的 $\delta^{18}O$ 值,部分 $\delta^{18}O$ 值略有升高(图 6)。华北克拉通锆石 $\delta^{18}O$ 范围为+1.47‰ ~ +8.93‰。卡普瓦尔克拉通锆石 $\delta^{18}O$ 范围为+3.9‰ ~ +7.4‰。达尔瓦克拉通锆石 $\delta^{18}O$ 值在+4.14‰ ~ +6.51‰之间,平均为+5.15‰。尽管许多锆石 $\delta^{18}O$ 值与地幔熔体处于平衡状态,但部分锆石 $\delta^{18}O$ 值较高($\delta^{18}O$ 为+8.93‰)(图 6),说明存在上地壳物质熔融或混染。部分高 $\delta^{18}O$ 值分布在太古宙岩浆锆石范围以上,表明玄武岩源经历了一定的低温蚀变,或发生地壳混染。大多数锆石具有一致的 Hf 同位素组成。这些观测结果与大规模岩浆活动对高 $\delta^{18}O$ 沉积岩的同化作用不一致,因为同化作用会导致初始 ε_{Hf} 值发生较大变化。由此可见,华北克拉通和卡普瓦尔克拉通 3.1 Ga 左右岩石中至少有一部分源岩在熔融前经历了低温蚀变而产生 TTG 熔体。特别是 3.1 Ga 左右华北克拉通锆石,$\delta^{18}O$ 值低至+1.47 ‰。它们可能记录了 3.1 Ga 左右岩浆混合作用事件的原始同位素特征。综上所述,3.1 Ga 左右岩浆锆石 $\delta^{18}O$ 变化范围较大,成因各不相同,3.1 Ga 左右地壳演化过程可能比之前认为的更为复杂。

4　3.1 Ga 左右岩石的地球化学特征

现有数据表明,主量元素氧化物如 TiO_2、Fe_2O_3、MnO、MgO、CaO、P_2O_5 与 SiO_2 之间存在明显负相关性(图 7)。能够反应压力变化的 Al_2O_3 与 SiO_2 之间存在微弱负相关关系。Na_2O、K_2O 与 SiO_2 之间存在明显正相关性。值得注意的是,印度地区 3.1 Ga 左右岩石存在 SiO_2 含量低、MgO 含量高的英云闪长质岩石,其稀土总量高,轻重稀土没有明显分异,存在较强 Eu 负异常。结合该区其他同时代岩石特征,这些英云闪长岩可能是基性岩浆结晶分异形成。华北克拉通的 TiO_2、MgO、Fe_2O_3 值普遍更高,而 MnO

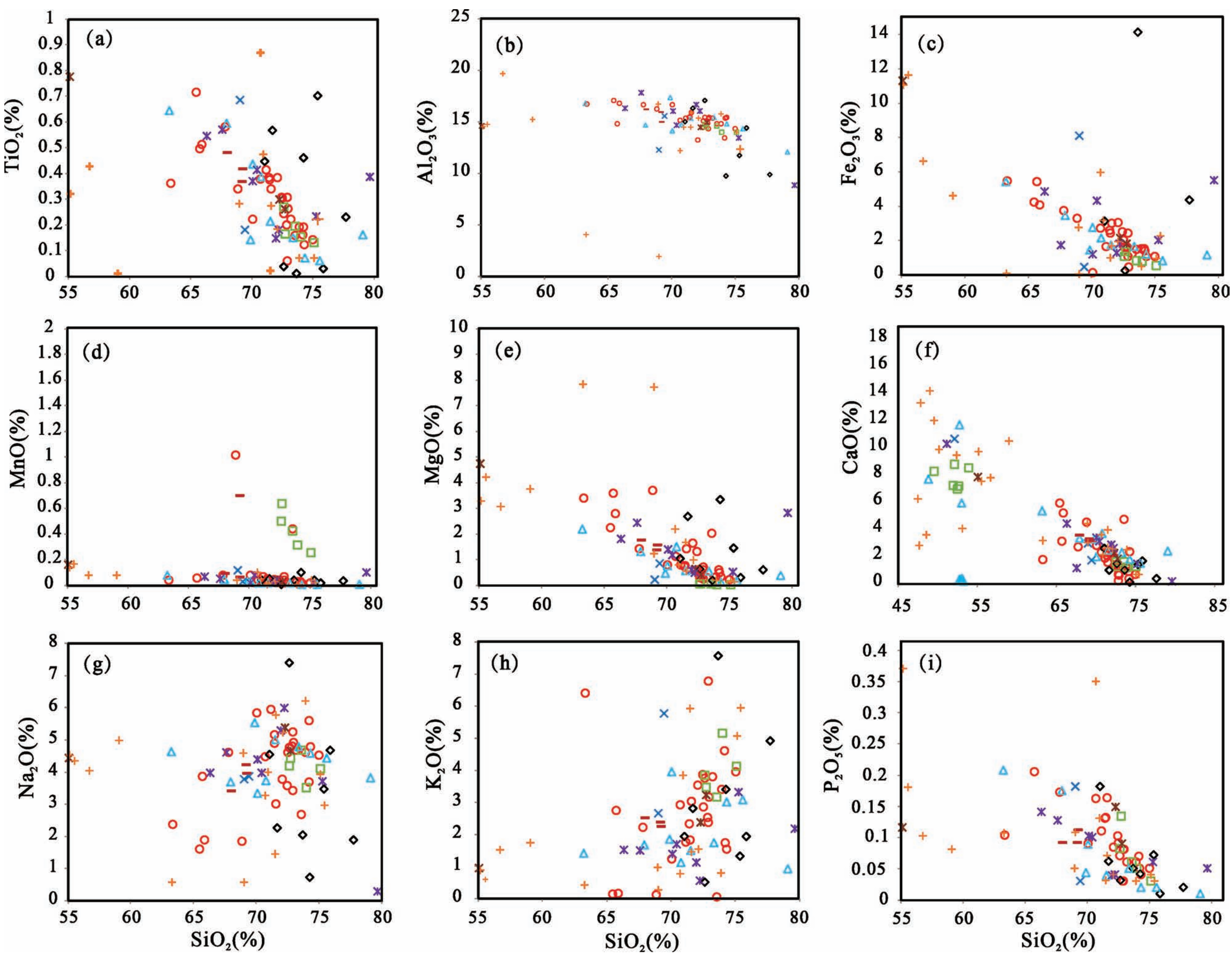

图 7 全球典型地区约 3.1 Ga 岩石哈克图解(数据来源同图 2;图例同图 4)

Fig. 7 Harker diagrams for selected major elements of the ~3.1Ga rocks (source of data same as Fig. 2;figure legend same as Fig. 4)

值与其他地区相似(图 7),且明显低于皮尔巴拉克拉通岩石样品,其余主要元素氧化物具有相同的分布趋势。

稀土元素是反映岩浆源区性质、岩浆起源与演化过程的良好地球化学指标。华北克拉通、皮尔巴拉克拉通、亚马逊克拉通、刚果克拉通和西南格陵兰部分地区的稀土元素配分样式基本相同(图 8),呈现出明显右倾趋势,表明轻稀土元素比较富集,而重稀土元素相对亏损,显示出强烈分馏的稀土配分模式。此外,铕存在轻微负异常,说明 TTG 岩浆经历了少量斜长石分离结晶。这些相似特征可能暗示这些地区的岩石可能具有相似的源区、成因模式和构造背景。相比之下,印度和西南格陵兰部分地区样式与其他地区有所不同,轻重稀土分异不明显,具有较为强烈铕正异常。由此可见,3.1 Ga 左右岩石在全球表现出明显差异,TTG 岩石形成过程显示出明显多样性,岩浆作用过程十分复杂,表明该时期陆壳的演化程度相对较高。

3.1 Ga 左右 TTG 岩石微量元素原始地幔标准化蛛网图如图所示(图 9)。图中数据显示出,中国三个主要克拉通、澳大利亚四个主要克拉通、非洲两个主要克拉通、西南格陵兰大部分地区、南美洲两个主要克拉通和西伯利亚克拉通的 3.1 Ga 左右岩石整体呈现出 Th、U、K、Pb 明显富集,Nb、Ta、P、Sm、Ti

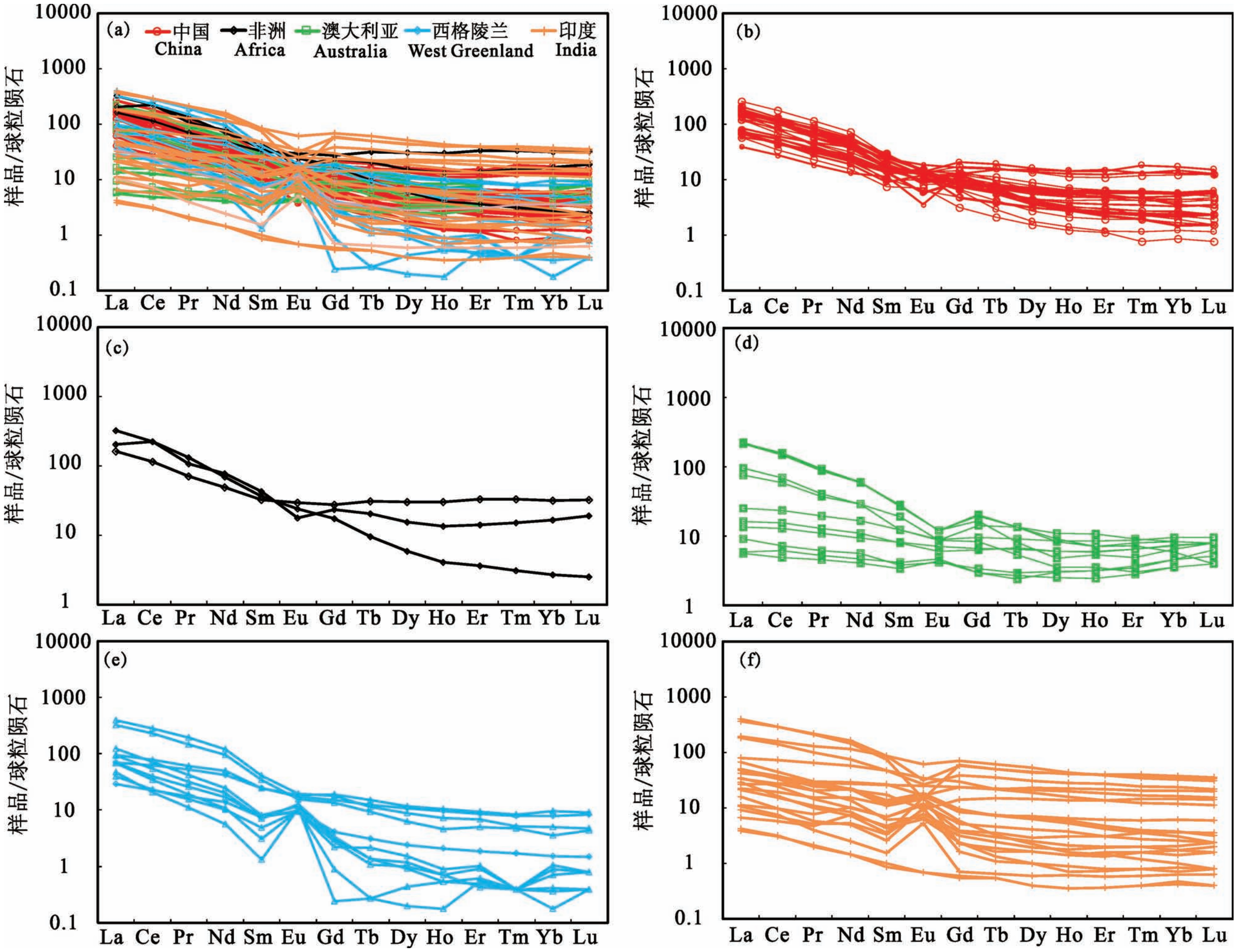

图 8 全球典型地区 3.1 Ga 左右岩石稀土元素配分图;(a)全球 3.1 Ga 左右 TTG 岩石稀土元素配分图;(b)中国地区 3.1 Ga 左右 TTG 岩石稀土元素配分图;(c)非洲地区 3.1 Ga 左右 TTG 岩石稀土元素配分图;(d)澳大利亚地区 3.1 Ga 左右 TTG 岩石稀土元素配分图;(e)西格陵兰地区 3.1 Ga 左右 TTG 岩石稀土元素配分图;(f)印度地区 3.1 Ga 左右 TTG 岩石稀土元素配分图(球粒陨石数据来自 Sun and McDonough, 1989)

Fig. 8 REE distribution patterns of the ~3.1Ga rocks from the word:(a) global REE distribution patterns for ~3.1Ga rocks;(b) REE distribution patterns of the ~3.1Ga rocks in China;(c) REE distribution patterns of the ~3.1Ga rocks in Africa;(d) REE distribution patterns of the ~3.1Ga rocks in Australia;(e) REE distribution patterns of the ~3.1Ga rocks in West Greenland;(f) REE distribution patterns of the ~3.1Ga rocks in India (The chondrite values are from Sun and McDonough, 1989)

相对亏损,显示出明显的岛弧配分样式。北美洲怀俄明克拉通则表现出 Ba、Ce、Ti 相对亏损和 Nb、Ta、Pb 相对富集的特征。印度四个主要克拉通则显示出 Ba、Nb、Pb 亏损和 Th、Ta、Hf 等元素富集。这进一步说明该时期 TTG 岩石的形成条件和构造背景呈现出多样性。

La/Yb 和 Sr/Y 比值被认为是反应 TTG 岩石形成压力的重要参数。在 3.1 Ga 左右岩石样品中,

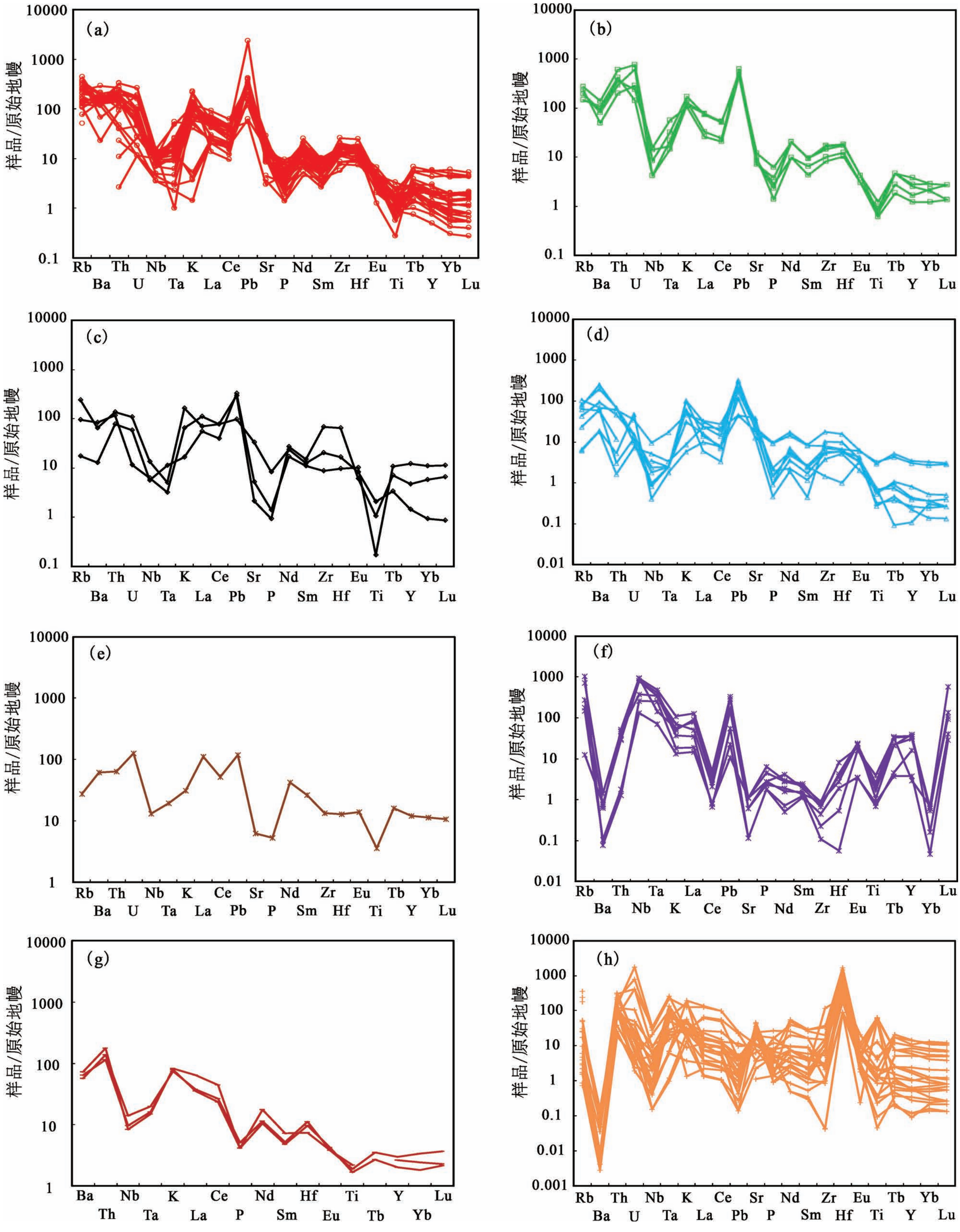

图 9 全球典型地区 3.1 Ga 左右 TTG 岩石原始地幔标准化微量元素蛛网图：(a) 中国；(b) 澳大利亚；(c) 非洲地区；(d) 西格陵兰地区；(e) 南美洲地区地区；(f) 北美洲地区；(g) 欧洲地区；(h) 印度。(地幔标准化数据来自 Sun et al., 1989)

Fig. 9 Primitive mantle normalized trace elements spidergrams for ~3.1 Ga TTG rocks from the world: (a) China; (b) Australia; (c) Africa; (d) the west Greenland region; (e) the South American region; (f) the North American region; (g) European region; (h) Indian region (The primitive mantle values are from Sun and McDonough, 1989)

Sr/Y 的比值位于 0~479 之间，Y 的值位于 0~43.9×10^{-6} 之间，呈现出较大变化范围。然而，大多数样品 Sr/Y 比值小于 120 且 Y 值小于 50×10^{-6}，这表明 3.1 Ga 左右 TTG 岩石多形成于中—低压条件下，但也有少数岩石表现出高压的特征。岩石样品的 La/Yb(1~1088)、Ce/Sr(1~473)值变化范围同样较大。从众多地球化学元素的比值变化可以看出，全球各地区 3.1 Ga 左右岩石的成因与形成环境是由巨大差距的，结合图 10c、d，可以说 3.1 Ga 左右 TTG 岩石的形成条件与构造背景十分复杂，并非均处于相同的构造机制之下。

综上所述，全球 3.1 Ga 左右 TTG 岩石 SiO_2 平均含量为 65.5%，MgO 平均含量为 4.4%，同时 MgO、Ni、Cr 值比较低，$Mg^{\#}$ 值中等偏高，Sr 值为中等程度等主微量数据，这些特征表明 3.1 Ga 左右 TTG 岩石可能来自玄武质岩石源区，部分源区发生低温蚀变。源区为约 3.3 Ga 时期从轻度亏损的地幔部分熔融形成。

5 3.1 Ga 左右岩浆事件与地壳生长

5.1 3.1 Ga 左右岩浆事件

陆壳大规模生长的主要过程为地幔提取玄武质岩浆，玄武质岩石部分熔融形成 TTG 岩石，TTG 岩石通过壳内再循环形成壳源花岗岩(Moyen et al., 2011)。根据已有资料显示，全球 20 余个太古宙克拉通发现了 3.1 Ga 左右锆石，10 余个克拉通中发现了 3.1 Ga 左右岩石。根据岩石锆石年龄分布图，已发现岩石的年龄在 3000~3200 Ma 间连续分布，有两个明显年龄峰值，分别为 3.15 Ga 和 3.05 Ga。其中 3.15 Ga 峰在全球范围内都有体现(南美洲除外)，这说明 3.15 Ga 岩浆事件是一次全球性质事件。全球 3.1 Ga 左右岩石 Hf 同位素数据显示，多数锆石具有正 $\varepsilon_{Hf}(t)$ 值和与锆石结晶年龄接近(年龄差<200Ma)的模式年龄，这说明 3.1 Ga 左右时期全球确实发生了一次全球性地壳生长。同时，部分锆石 $\varepsilon_{Hf}(t)$ 为负值，并且具有与锆石结晶年龄相差较远的模式年龄，说明 3.1 Ga 左右时期不仅是新生地壳生长，同时也发生了古老地壳物质重熔。

根据现有地壳年龄数据，学者们提出了多种地壳生长曲线。从图 11a 中可以看出，在部分学者提出的地壳生长曲线中，3.1 Ga 左右时期地壳生长速率或多或少存在转折趋势，说明地壳生长演化在该时期发生了变化。同时，在大陆曲线相关图(图 11b)中，地壳改造速率在该时期呈现下降趋势，地幔温度开始下降，地壳厚度由下降趋势转变为上升趋势，这支持了部分学者的观点，即地壳的形成机制在 3.2~3.0 Ga 期间发生明显转变，从垂向生长逐渐过渡为水平生长(Dhuime et al., 2015; Hawkesworth et al., 2020; Johnson et al., 2019; Chowdhury et al., 2020)。

综上所述，约 3.1 Ga 发生了一次较大规模的地壳增生事件。

5.2 3.1 Ga 左右构造环境

前人研究表明，3.1 Ga 左右时期的 TTG 岩石可能是在不同构造背景下通过不同过程形成的(Palin et al., 2016)，包括交代重力差异沉降、热管构造和滞留盖构造、俯冲洋壳和加厚弧中变质玄武岩(角闪岩)的熔融(Nagel et al., 2012; Polat et al., 2015; 徐楠等, 2023)。这些成因可以概括为两种认识：① 板片俯冲到地壳之下后，板片熔融形成；② 深部地壳物质部分熔融形成。Dhuime 等(2015)通过研究 13125 个来源和地质状况未知的火山岩和深成岩样品的组成，提出了新生地壳的 Rb/Sr 比值在 3.2~3.0 Ga 急剧增加的认识(Dhuime et al., 2015)。Johnson 等(2019)研究表明太古宙 TTG 中 K_2O/Na_2O、Sr/Y 和 La_N/Yb_N 比值在 3.3~3.0 Ga 过渡时期发生显著变化。这些结果表明 3.3~3.0Ga 之间全球构造可能发生了根本的转变，从非板块构造停滞—盖层状态到移动—盖层状态(Dhuime et al., 2015; Hawkesworth et al., 2020; Johnson et al., 2019; Chowdhury et al., 2020)。然而，有学者认为，这种变化也可能是地壳长期冷却而导致相容和不相容元素浓度发生重大变化的结果，而不是地壳主要成分变化或构造样式发生变化的结果(Keller et

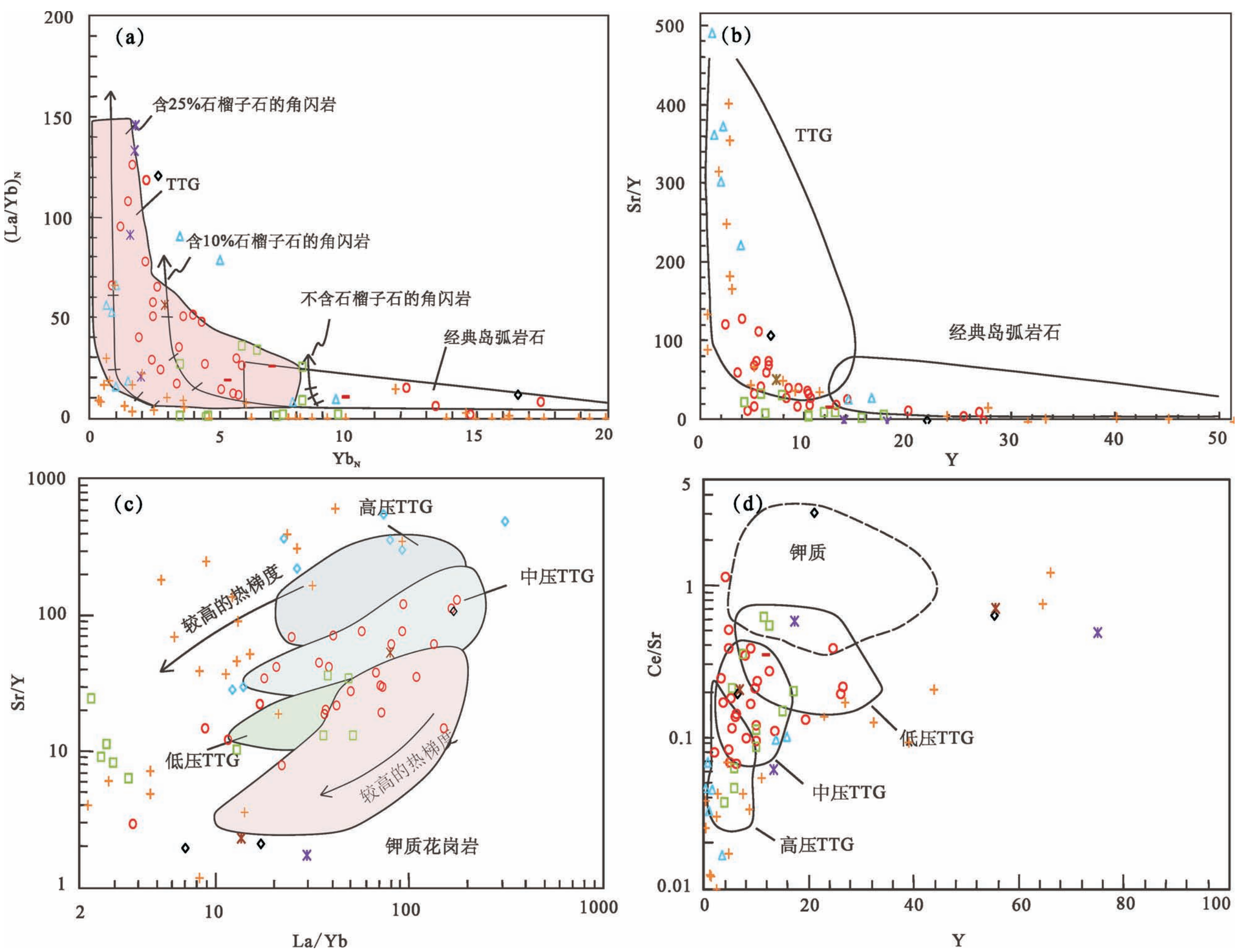

图 10 (a) Yb_N—$(La/Yb)_N$ 图解(底图据 Wan et al., 2005);(b) Y—Sr/Y 图解(底图据 Zheng Jianpeng et al., 2009);(c) La/Yb—Sr/Y 图解(底图修改自 Moyen et al., 2011);(d) Y—Ce/Sr 图解(底图修改自 Moyen et al., 2011)(图例同图 4)

Fig. 10 (a) Yb_N vs. $(La/Yb)_N$ diagram (after Wan et al., 2005); (b) Y vs. Sr/Y diagram (after Zheng Jianpeng et al., 2009), (c) La/Yb vs. Sr/Y diagram (after Moyen et al., 2011). (d) Y vs. Ce/Sr diagram (after Moyen et al., 2011) (figure legend same as Fig. 4)

al., 2020;Windley et al., 2021)。

中太古代 Ivisaartoq(西格陵兰)和新太古代 Schreiber—Hemlo 绿岩带(加拿大)太古宙火山岩岩浆期后元素活动性及微量元素研究表明变质过程使微量元素在某些岩性中丢失,同时在其他岩性中得到,具有广泛的互补性(Ordóñez-Calderón et al., 2008;Polat et al., 2012)。然而,在 3.1 Ga 左右岩石的微量元素数据均只有显示 Pb 正异常,没有 Pb 亏损,这表明 Pb 正异常并不是后期变质作用的结果。结合 Th、U、K 元素明显富集,Nb、Ta、P、Sm、Ti 元素相对亏损特征,3.1 Ga 左右岩石的形成与可能俯冲作用密切相关。Hildebrand 等人(2018)指出 TTG 自 3.8 Ga 以来主要来自板片熔融而不是加厚的弧岩浆,由此便有了古太古代以来俯冲作用就已经开始的观点(Hildebrand et al., 2018)。

然而,俯冲作用无法完全解释 3.1 Ga 左右 TTG 岩石和绿岩带的一些特征:

(1)如果俯冲过程导致新地壳形成,那么在不同区域可能会识别出不同的年龄峰,从而形成一个全球年龄的连续。然而,在 3.1 Ga 左右时期,全球克拉通基底 70%左右为 TTG 侵入体,这些侵入体几乎同时侵入了当时存在的各个古陆核,这是俯冲作用无法解释的。

(2)全球太古宙克拉通典型构造是穹隆构造,

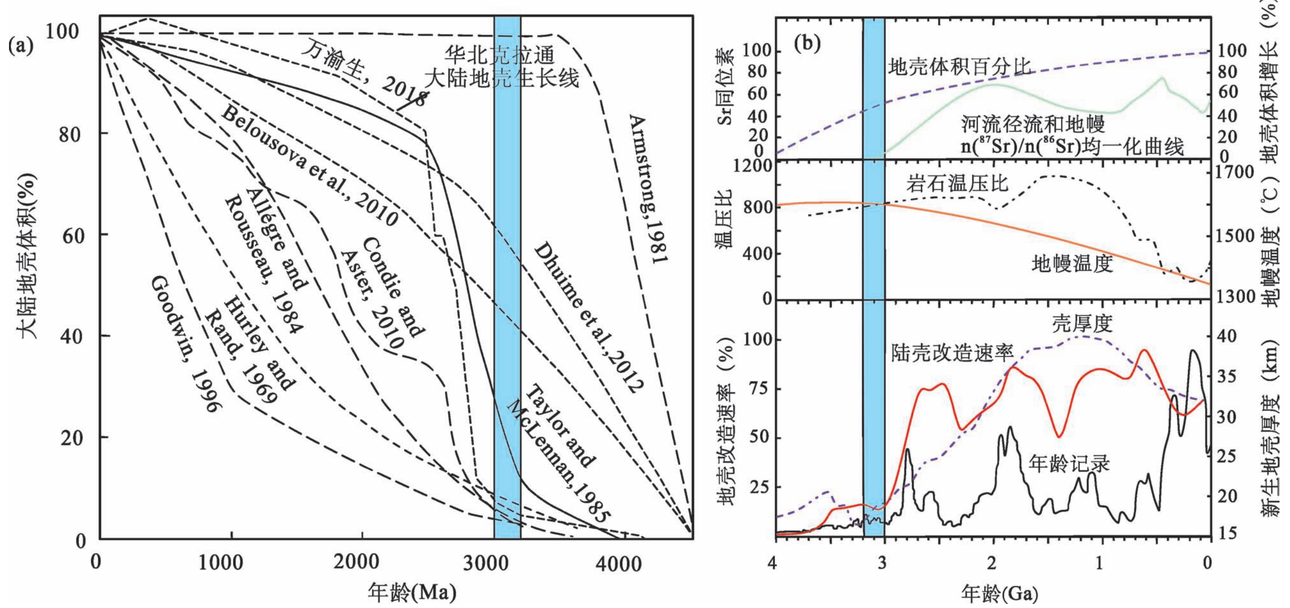

图 11 大陆地壳体积生长线(底图修改自万渝生等,2022)和大陆生长相关曲线(底图修改自樊海龙等,2023)

Fig. 11 The global crustal growthcurves(after Wan Yusheng et al., 2022&) and Crustal growth curves (after Fan Hailong et al., 2023&)

主要是由 TTG 岩石底辟形成,与俯冲带形成的大规模逆冲带、线性构造带、韧性剪切带等构造样式有所不同。

(3)3.1 Ga 左右时期尚未发现确定俯冲带存在的重要标志——双变质带。尽管在地球化学上发现俯冲带存在的一些证据,但野外地质记录却不相符。因此,越来越多的学者认为,地球早期存在的长英质大陆是某种前板块构造体制下的产物(Hamilton et al., 2011,2019;Brown et al., 2020)。

综合前人研究,3.1 Ga 左右时期全球地壳演化机制存在垂向生长和水平演化两种机制的并行。深部地壳部分熔融是地壳演化的重要过程,其形成机制因不同构造单元和地质背景而异。部分地区花岗岩具有相对平坦的 HREE 模式,以及高 Zr/Sm、低 Gd/Yb、Dy/Yb、Nb/Ta 值说明岩石主要由古老地壳部分熔融而来,并且这些 TTG 片麻岩样品具有低 Mg# 值,以及极低的 Cr 和 Ni 浓度,这排除了地幔物质为岩浆来源做出贡献的可能性,并表明 TTG 岩浆可能是由早期存在的地壳岩石部分熔化形成的,而不是俯冲的海洋地壳形成的(Ao Wenhao et al., 2021)。与此类似的地区还有圣弗朗西斯科克拉通 Gavi ao 地块(Medeiros et al., 2017;Lopes et al., 2021)、西格陵兰岛基亚地体(Gardiner et al., 2019;Kirkland et al., 2020)、萨尔玛西亚克拉通东部花岗—绿岩带(Lobach-Zhuchenko et al., 2017)等。这些地区 3.1 Ga 左右 TTG 主要通过地幔柱影响地壳下部,下地壳部分熔融产生的。另有如高勒克拉通部分岩石因含放射性元素(如铀、钍)热量释放而熔融,而非因地幔柱的影响而产生的熔融(Fraser et al., 2010)。总体来说,深部地壳的部分熔融机制在不同地质环境下的表现是多样的,其主导因素包括构造背景、地幔热源以及地壳物质的组成。而其余地区具有高 LILE(大离子亲石元素) 浓度、富 Nb 和 Ta 浓度(以及 Nb/La 比率)高于典型的岛弧和大陆玄武岩、$\varepsilon_{Hf}(t)$ 值具有幔源特征等类似现代大洋岛弧的地球化学特征认为是在早期衍生的洋壳俯冲到早期陆壳下形成,类似的构造环境也在西达瓦克拉通 Nugggihalli 绿岩带(Sameer et al., 2020)、库尔格地块(Yu Bing et al., 2022;Anoop et al., 2021)、圣弗朗西斯科克拉通南部绿岩带(Marimon et al., 2022)、怀俄明克拉通(Smithies et al., 2003)等地区得到表现,均显示出与岛弧或俯冲背景相关的地球化学特征。另有地区记录了近陆相扇组合—水下三角洲前缘组合—浅海陆架的沉积环境,表明这些地区可能与古代洋壳俯冲及岛弧活动密切相关(De et al., 2020;Sindhuja et al., 2022)。总体而言,以上地区的地质证据表明,俯冲板片部分熔融在这些区域的地壳演化中扮演了关键角色。其岩浆活动与岛

弧形成、洋壳俯冲等环境密切相关,表明在地球早期,俯冲板块是推动地壳动态演化的重要因素。

总体来看,3. 1 Ga 左右岩石的成因呈现多样性,包括俯冲作用导致的板块边缘增生和洋底高原加厚下地壳部分熔融。下地壳部分熔融在大部分地区都是存在的,而板块俯冲只在少量地区起作用。这说明至少在 3. 1 Ga 左右时,某种形式的板块构造运动已经在地球上开始,但此时起主导作用的构造样式仍然是地幔柱主导的垂向构造。

6　总结

(1)全球各个地区 TTG 岩石的资料表明,中太古代(3. 15Ga 和 3. 0Ga)发生了两次全球性的岩浆活动。3. 1 Ga 左右岩石遍布全球各个大陆,现今主要集中在北半球,南半球数量较少。岩石普遍遭受后期变质作用改造形成片麻岩,原始岩石几乎不可见。3. 1 Ga 左右岩石以英云闪长岩和奥长花岗岩为主,呈现出过铝质的特征。华北克拉通、塔里木、印度库格地块等地发现有高级变质作用形成的麻粒岩,皮尔巴拉、库格地块和萨尔玛提亚等克拉通中发现有流纹岩和凝灰岩等火山岩,具有一定的地区独特性。

(2)中国、澳大利亚、非洲、西南格陵兰、南美洲和西伯利亚克拉通的 3. 1 Ga 左右岩石整体呈现出轻稀土富集,重稀土亏损的右倾模式,铕明显异常;微量元素整体存在 Th、U、K、Pb 相对富集,Nb、Ta、P、Sm、Ti 相对亏损,北美洲怀俄明克拉通和印度主要克拉通微量元素与其他地区有明显差异。全球 3. 1 Ga 左右锆石的 $\varepsilon_{Hf}(t)$ 具有明显差异;同一地区的锆石 Hf 同位素组成也有明显差异。大部分锆石 $\delta^{18}O$ 值与地幔熔体处于平衡状态(+5. 3±0. 6‰),但也有部分锆石 $\delta^{18}O$ 值较高,达+8. 93‰,可能表示上地壳物质的熔融。

(3)3. 2~3. 0Ga 时期岩石组合、全岩地球化学和锆石 O—Hf 同位素在各个克拉通上存在差异,表明该时期岩浆作用过程十分复杂,地壳生长的机制可能是垂向和水平演化两种方式并行。

参　考　文　献　/　References

(The literature whose publishing year followed by a “&” is in Chinese with English abstract; The literature whose publishing year followed by a “#” is in Chinese without English abstract)

邓晋福,冯艳芳,狄永军,刘翠,肖庆辉,苏尚国,赵国春,孟斐,马帅,姚图. 2015. 岩浆弧火成岩构造组合与洋陆转换. 地质论评, 61(3): 473 ~ 484.

邓晋福,刘翠,冯艳芳,肖庆辉,狄永军,苏尚国,赵国春,段培新,戴蒙. 2015. 关于火成岩常用图解的正确使用:讨论与建议. 地质论评, 61(4): 717 ~ 734.

董春艳,万渝生,张玉海, 杨之青, 刘敦一. 2013. 鞍山地区东山杂岩 3. 3~3. 1Ga 岩浆作用:地球化学和锆石 SHRIMP 定年. 岩石学报,29(02):414 ~ 420.

樊海龙,杨高学,郭建明,马雪云,刘翔. 2023. 地球早期大陆地壳的形成与演化. 地质论评,69(02):669~690.

郭新成, 郑玉壮, 高军, 朱志新. 2013. 新疆西昆仑中太古界古陆核的确定及地质意义. 地质论评,59(03):401 ~ 412.

邱啸飞,陈伟雄,徐大良,赵小明,董喜润. 2022. 扬子陆核崆岭杂岩太古宙地壳演化. 华南地质,38(01):56 ~ 66.

孙会一,颉颃强,刘守偈,董春艳, 刘敦一, 万渝生. 2016. 冀东黄柏峪—羊崖山地区太古宙岩浆作用和变质作用——SHRIMP 锆石 U-Pb 定年. 地质通报,35(01):27 ~ 42.

万渝生,董春艳,颉颃强,李源,王宇晴,王堃力. 2022. 华北克拉通新太古代早期—中太古代晚期(2. 6~3. 0 Ga)巨量陆壳增生:综述. 地质力学学报, 28(05): 866 ~ 906.

万渝生,颉颃强,王惠初,李鹏川,初航,肖志斌,董春艳,刘守偈,李源,郝光明,刘敦一. 2021. 冀东地区~3. 8 Ga TTG 岩石发现. 地质学报,95(05):1321 ~ 1333.

万渝生,宋彪,刘敦一,李惠民,杨淳,张巧大,杨崇辉,耿元生,沈其韩. 2001. 鞍山东山风景区 3. 8~2. 5Ga 古老岩带的同位素地质年代学和地球化学. 地质学报,3:363 ~ 370.

王德英,王清斌,刘晓健,赵梦,郝铁伟. 2019. 渤海湾盆地海域片麻岩潜山风化壳型储层特征及发育模式. 岩石学报,35(04):1181 ~ 1193.

吴鸣谦,左梦璐,张德会,赵国春. 2014. TTG 岩套的成因及其形成环境. 地质论评, 60(3): 503 ~ 514.

徐楠,吴才来,赵苗苗,刘畅. 2023. 茫崖闪长岩的成因及对造山带构造演化的指示意义. 地质论评, 69(6): 2085 ~ 2111.

张金朋,汪洋. 2024. 识别富斜长石花岗岩类的岩石化学图解:评价与辨析. 地质论评, 70(5): 1963 ~ 1980.

张旗,原杰. 2024. 地球化学研究的危机与机遇. 地质论评, 70(5): 1907 ~ 1926.

张世红,王鸿祯. 2002. 古大陆再造的回顾与展望. 地质论评, 48(2): 198 ~ 213.

张拴宏,赵越,裴军令,王宏宇,胡国辉,张琪琪,蔡瑜杭,孔令昊,王森,王开. 2022. 大火成岩省及其在古大陆重建及裂解研究中的应用. 地质论评, 68(5): 1634 ~ 1652.

赵燕,第五春荣,敖文昊,王洪亮,朱涛,孙勇. 2015. 敦煌地块发现~3. 06 Ga 花岗闪长质片麻岩. 科学通报,60(01):75 ~ 92.

周红英,刘敦一,万渝生,Wilde S A, 伍家善. 2007. 鞍山地区 3 . 3 Ga 岩浆热事件——SHRIMP 年代学和地球化学新证据. 岩石矿物学杂志,106(02):123 ~ 129.

周红英,刘敦一,万渝生. 2008. 辽宁鞍山地区东山杂岩带 3. 3~3. 1Ga 期间的岩浆作用——锆石 SHRIMP U-Pb 定年. 地质通报, 27(12):2122 ~ 2126.

Adhikari A, Vadlamani R. 2022. Petrogenesis of the Mesoarchean (~3. 05Ga) mafic volcanics from the western Iron Ore Group volcano—sedimentary succession, Singhbhum craton, eastern India: Constraints from geochemical modelling and Sm-Nd geochronology. Lithos, 412: 106596.

Akame J M, Owona S, Hublet G, Debaille V. 2020. Archean tectonics in the sangmelima granite—greenstone terrains, Ntem Complex (NW Congo craton), southern Cameroon. Journal of African earth sciences, 168: 103872.

Almeida J D A C D, Dall' Agnol R, Oliveira M A, Macambira M J B, Pimentel M M, Rämö O T, Guimarães F V, Leite A A D S. 2011. Zircon geochronology, geochemistry and origin of the TTG suites of the Rio Maria granite—greenstone terrane: Implications for the growth of the Archean crust of the Carajás province, Brazil. Precambrian Research, 187(1~2): 201 ~ 221.

Almeida J D A C D, Dall'Agnol R, Leite A A D S. 2013. Geochemistry and zircon geochronology of the Archean granite suites of the Rio Maria granite—greenstone terrane, Carajas Province, Brazil. Journal of South American Eaeth Sciences, 42: 103 ~ 126.

Amaldev T, Santosh M, Li Tang, Baiju K R, Tsunogae T, Satyanarayanan M. 2016. Mesoarchean convergent margin processes and crustal evolution: Petrologic, geochemical and zircon U-Pb and Lu-Hf data from the Mercara Suture Zone, southern India. Gondwana Research, 37: 182 ~ 204.

Anoop K S, Anilkumar Y, Santosh M, Yu Bing, Joy K D, Kavvyanjali K V, Sathyan A, Mathew A, Sajinkumar K S. 2021. Magmatic and metamorphic evolution of a layered gabbro—anorthosite complex from the Coorg Block, southern India: Implications for Mesoarchean suprasubduction zone process. Gondwana Research, 103: 105 ~ 134.

Ao Wenhao, Zhai M, Zhao Yan, Zhang Chengli, Sun Yonggang, George P, Sajeev K, Gou Longlong, Lu Junsheng, Hu Yuhua. 2021. Paleo—Mesoarchean crustal growth and reworking in the western Dharwar Craton, southwestern India: Evidence from trondhjemitic gneiss and granitic gneiss. Precambrian Research, 367: 106428.

Armstrong R L. 1991. The persistent myth of crustal growth. Australian Journal of Earth Sciences, 38, 613 ~ 620.

Augé T, Cocherie A, Genna A, Armstrong R, Guerrot C, Mukherjee M M, Patra R N. 2003. Age of the Baula PGE mineralization (Orissa, India) and its implications concerning the Singhbhum Archaean nucleus. Precambrian Research, 121(1~2): 85 ~ 101.

BaoHan, Liu Shuwen, Wang Maojiang, Teng Guoxu, Sun Guozheng. 2020. Mesoarchean geodynamic regime evidenced from diverse granitoid rocks in the Anshan—Benxi area of the North China Craton. Lithos, 366: 105574.

Barbosa N, Menezes Leal A B, Debruyne D, Bastos Leal L R, Barbosa N, Marinho M, Merces L, Barbosa J, Koproski L M. 2020. Paleoarchean to Paleoproterozoic crustal evolution in the Guanambi—Correntina block (GCB), north São Francisco Craton, Brazil, unraveled by U-Pb Geochronology, Nd—Sr isotopes and geochemical constraints. Precambrian Research, 340: 105614.

Barbosa R G, Ferreira A C D, Leitzke F, Santos T N D, Conceição R, Martin H. 2023. A review of 3.66 to 2.77 Ga crustal differentiation in the northern Sao Francisco Craton, Brazil. International Geology Review, 65: 1541 ~ 1557.

Belcher R W, Afm K. 2006. Syntectonic emplacement and deformation of the Heerenveen batholith: Conjectures on the structural setting of the 3.1 Ga granite magmatism in the Barberton granite—greenstone terrain, South Africa. Japanese Journal of Health & Human Ecology, 405(8): 211 ~ 231.

Bhaskar R Y J, Beck W, Rama M V, Nirmal C S, Naqvi S M. 1983. Geology, geochemistry and age of metamorphism of Archaean grey gneisses around Channarayapatna, Hassan District, Karnataka, South India. Memoirs of the Geological Survey of India, 4: 309 ~ 328.

Bibikova E V, Lobach-Zhuchenko S B, Artemenko G V, Claesson S, Kovalenko A V, Krylov I N. 2008. Late Archean magmatic complexes of the Azov terrane, Ukrainian Shield: Geological setting, isotopic age, and sources of material. Petrology 16: 211 ~ 231.

Bickford M E, Wooden J L, Bauer R L. 2006. SHRIMP study of zircons from Early Archean rocks in the Minnesota River Valley: Implications for the tectonic history of the Superior Province. Geological Society of America Bulletin, 118(1~2): 94 ~ 108.

Bizzarro M, Simonetti A, Stevenson R K, David J. 2002. Hf isotope evidence for a hidden mantle reservoir. Geology, 30: 771 ~ 774.

Boger S D, Maas R, Fanning C M. 2008. Isotopic and geochemical constraints on the age and origin of granitoids from the central Mawson Escarpment, southern Prince Charles Mountains, East Antarctica. Contributions to Mineralogy & Petrology, 155(3): 379 ~ 400.

Boger S D, Wilson C J L, Fanning C M. 2006. An Archaean province in the southern Prince Charles Mountains, East Antarctica: U-Pb zircon evidence for c. 3170Ma granite plutonism and c. 2780Ma partial melting and orogenesis. Precambrian Research, 145: 207 ~ 228.

BöHm C O, Heaman L M, Stern R A, Coekery M T, Creaser R A. 2003. Nature of assean lake ancient crust, Manitoba: a combined SHRIMP-ID-TIMS U-Pb geochronology and Sm-Nd isotope study. Precambrian Research, 126(1~2): 55 ~ 94.

Bosch D, Bruguier O, Pidgeon R, 1996. Evolution of an Archean metamorphic belt: A conventional and SHRIMP U-Pb study of accessory. Journal of Geology, 104: 695 ~ 711.

Brown M, Johnson T, Gardiner N. 2020. Plate Tectonics and the Archean Earth. Annual Review of Earth and Planetary Sciences, 48: 291 ~ 320.

Chakraborti T M, Ray A, Deb G K, Upadhyay D, Chakrabarti R. 2019. Evidence of crustal reworking in the Mesoarchean: Insights from geochemical, U-Pb zircon and Nd isotopic study of a 3.08~3.12Ga ferro—potassic granite-gneiss from north-eastern margin of Singhbhum Craton, India. Lithos, 330~331: 16 ~ 34.

Chen Shefa, Riganti A, Wyche S, Greenfield J E, Nelson D R. 2003. Lithostratigraphy and tectonic evolution of contrasting greenstone successions in the central Yilgarn Craton, Western Australia. Precambrian Research, 127(1~3): 249 ~ 266.

Chernyshov N M, Ryborak M V, Al'bekov A Y. 2014. Isotopic and geochemical evidence for the process of mantle—crust interaction in formation of the Late Archean greenstone belts of Kursk Block of Sarmatia. Mineralogicheskii Journal, 2014, 36(2): 92 ~ 101.

Chowdhury P, Chakraborty S, Gerya T V, Cawood P A, Capitanio F A. 2020. Peel-back controlled lithospheric convergence explains the secular transitions in Archean metamorphism and magmatism. Earth and Planetary Science Letters, 538: 116224.

Condie K C, Aster R C. 2010. Episodic zircon age spectra of orogenic granitoids: the supercontinent connection and continental growth. Precambrian Res, 180: 227 ~ 236.

Corfu F. 1988. Differential response of U-Pb systems in coexisting accessory minerals, Winnipeg River Subprovince, Canadian Shield: implications for Archean crustal growth and stabilization. Mineral and Petrol, 98: 312 ~ 325.

Cui Xiaozhuang, Wang Jian, Sun Zhiming, Wang Wei, Deng Qi, Ren Guangming, Liao Shiyong, Huang Mingda, Chen Fenglin, Ren Fei. 2018. Early Paleoproterozoic (ca. 2.36Ga) post-collisional granitoids in Yunnan, SW China: Implications for linkage between Yangtze and Laurentia in the Columbia supercontinent. Journal of Asian Earth Sciences, 169: 308 ~ 322.

Cui Xiaozhuang, Wang Jian, Wang XuanCe, Wilde S A, Ren Guangming, Li Shaojie, Deng Qi, Ren Fei, Liu Junping. 2021. Early crustal evolution of the Yangtze Block: Constraints from zircon U—Pb—Hf isotope systematics of 3.1~1.9 Ga granitoids in the

Cuoke Complex, SW China. Precambrian Research, 357: 106155.
Dai Yanpei, Zhang Lianchang, Zhu Mingtian, Wang Changle, Liu Li, Xiang Peng. 2014. The composition and genesis of the Mesoarchean Dagushan banded iron formation (BIF) in the Anshan area of the North China Craton. Ore Geology Reviews, 63: 353 ~ 373.
Dantas E L, Van Schmus W R, Hackspacher P C, Fetter A H, Neves B B D B, COrdani U, Nutman A P, Williams I S. 2004. The 3. 4~3. 5 Ga São José do Campestre massif, NE Brazil: remnants of the oldest crust in South America. Precambrian Research, 130(1~4): 113 ~ 137.
Dasgupta A, Bhowmik S K, Dasgupta S, Avila J, Ireland T R. 2019. Mesoarchaean clockwise metamorphic P—T path from the Western Dharwar Craton. Lithos: An International Journal of Mineralogy, Petrology, and Geochemistry, 342~343: 370 ~ 390.
Davis D W, Sutcliffe R H, Trowell N F. 1988. Geochronological constraints on the tectonic evolution of a late Archaean greenstone belt, Wabigoon Subprovince, Northwest Ontario, Canada. Precambrian Research, 39(3): 171 ~ 191.
De S. 2020. Alluvial fan to shallow marine sedimentation record in the ~3. 0Ga Keonjhar Quartzite, Singhbhum Craton, India: An example of Phanerozoic style passive margin sedimentation from the Mesoarchean. Precambrian Research, 352: 105962.
Deng Jinfu, Feng Yanfang, Di Yongjun, Liu Cui, Xiao Qinghui, Su Shangguo, Zhao Guochun, Meng Fei, Ma Shuai, Yao Tu. 2015&. Magmatic Arc and Ocean—Continent Transition: Discussion. Geological Review, 61(3): 473 ~ 484.
Deng Jinfu, Liu Cui, Feng Yanfang, Xiao Qinghui, Di Yongjun, Su Shangguo, Zhao Guochun, Dduan Peixin, Dai Meng. 2015&. On the Correct Application in the Common Igneous Petrological Diagrams: Discussion and Suggestion. Geological Review, 61(4): 717 ~ 734.
Dhuime B, Hawkesworth C J, Cawood P A, Storey C D. 2012. A Change in the Geodynamics of Continental Growth 3 Billion Years Ago. Science, 335: 1334 ~ 1336.
Dhuime B, Wuestefeld A, Hawkesworth C J. 2015. Emergence of modern continental crust about 3 billion years ago. Nature Geoscience, 8: 552 ~ 555
Dong Chunyan, Wan Yusheng, Zhang Yuhai, Yang Zhiqing, Liu Dunyi. 2013&. 3. 3 ~ 3. 1Ga magmatism recorded in an outcrop of the Dongshan Complex in the Anshan area, North China Craton: Evidence from geochemistry and SHRIMP zircon dating. Acta Petrologica Sinica, 29(2): 414 ~ 420.
Fan Hailong, Yang Gaoxue, Guo Jianming, Ma Xueyun, Liu Xiang. 2022&. The origin and evolution of earth's oldest continental crust. Geological Review, 68(5): 2022102002.
Fernandes C M D, Galarza M A, Teixeira de Gouvêa R C, Tavares de Souza H P. 2021. Geochemical, geochronological, and isotopic constraints for the Archean metamorphic rocks of the westernmost part of the Carajás Mineral Province, Amazonian Craton, Brazil. Journal of South American Earth Sciences, 110: 103340.
Fraser G, Neumann N, McAvaney S, Szpunar M, Reid A. 2010. Discovery of early Mesoarchean crust in the eastern Gawler Craton, South Australia. Precambrian Research, 179(1~4): 1 ~ 21.
Gamal El Dien H, Doucet L S, Murphy J B, Zheng XiangLi. 2020. Geochemical evidence for a widespread mantle re-enrichment 3. 2 billion years ago: implications for global-scale plate tectonics. Scientific Reports, 10: 9461.
Gao Lei, Liu Shuwen, Zhang Bo, Sun Guozheng, Hu Yalu Guo R. 2019. A Ca. 2. 8-Ga Plume-Induced Intraoceanic Arc System in the Eastern North China Craton. Tectonics, 38(5~6): 1694 ~ 1717.
Garde A A, Friend C R, Nutman A P, Marker M. 2000. Rapid maturation and stabilisation of middle Archaean continental crust: the Akia terrane, southern West Greenland. Bulletin of the Geological Society of Denmark, 47: 1 ~ 27.
Garde A A, Whitehouse M, Christensen R. 2012. Mesoarchean Epithermal Gold Mineralization Preserved at Upper Amphibolite-Facies Grade, Qussuk, Southern West Greenland. Economic Geology, 107 (5): 881~908.
Garde A A. 2007. A mid-Archaean island arc complex in the eastern Akia terrane, Godthåbsfjord, southern West Greenland. Journal of the Geological Society, 164(3): 565 ~ 579.
Gardiner N J, Kirkland C L, Hollis J, Szilas K, Steenfelt A, Yakymchuk C, Heide-Jørgensen H. 2019. Building Mesoarchaean crust upon Eoarchaean roots: the Akia Terrane, West Greenland. Contributions to Mineralogy and Petrology, 174(3): 20.
Gaucher G, Frei R, Chemale Jr F, Frei D, Bossi J, Martínez G, Chiglino L, Cernuschi F. 2011. Mesoproterozoic evolution of the Rio de la Plata Craton in Uruguay: at the heart of Rodinia? International journal of earth sciences: Geologische Rundschau, 100 (2~3): 273 ~ 288.
Ge Rongfeng, Simon A W, Zhu Wenbin, Zhou Teng, Si Yang. 2022. Formation and evolution of Archean continental crust: A thermodynamic—geochemical perspective of granitoids from the Tarim Craton, NW China. Earth-Science Reviews, 234: 104219.
Ge Rongfeng, Zhu Wenbin, Wu Hailin, Zheng Bihai, He Jingwen. 2013. Timing and mechanisms of multiple episodes of migmatization in the Korla Complex, northern Tarim Craton, NW China: Constraints from zircon U—Pb—Lu—Hf isotopes and implications for crustal growth. Precambrian Research, 231: 136 ~ 156.
Gifford J N, Mueller P A, Foster D A, Mogk D W. 2014. Precambrian crustal evolution in the Great Falls tectonic zone: insights from xenoliths from the Montana alkali province. Journal of Geology, 122: 531 ~ 548.
Gifford J N, Mueller P A, Foster D A, Mogk D W. 2018. Extending the realm of Archean crust in the Great Falls tectonic zone: Evidence from the Little Rocky Mountains, Montana. Precambrian Research, 315: 264 ~ 281.
Goodge J W, Fanning C M. 2016. Mesoarchean and Paleoproterozoic history of the Nimrod Complex, central Transantarctic Mountains, Antarctica: Stratigraphic revisions and relation to the Mawson Continent in East Gondwana. Precambrian Research, 285: 242 ~ 271.
Grace R L, Chamberlain K R, Frost B R, Frost C D. 2006. Tectonic histories of the Paleo- to Mesoarchean Sacawee block and Neoarchean Oregon Trail structural belt of the south—central Wyoming province. Canadian Journal of Earth Sciences, 43(10): 1445 ~ 1466.
Grew E S, Manton W I, James P R. 1988. U-Pb data on granulite facies rocks from fold island, Kemp Coast, East Antarctica. Precambrian Research, 42(1): 63 ~ 75.
Guitreau M, Mukasa S B, Loudin L, Krishnan S. 2017. New constraints on the early formation of the Western Dharwar Craton (India) from igneous zircon U-Pb and Lu—Hf isotopes. Precambrian Research, 302: 33 ~ 49.
Guo Xincheng, Zheng Yuzhaung, Gao Jun, Zhu Zhixin. 2013&. Determination and Geological Significance of the Mesoarchean Craton in Western Kunlun Mountains, Xinjiang, China. Geological Review, 59(3):401 ~ 412.
Hamilton W B. 2011. Plate tectonics began in Neoproterozoic time, and plumes from deep mantle have never operated. Lithos, 123: 1 ~

20.

Hamilton W B. 2019. Toward a myth-free geodynamic history of Earth and its neighbors. Earth-Science Reviews, 198: 102905.

Hawkesworth C J, Cawood P A, Dhuime B. 2020. The Evolution of the Continental Crust and the Onset of Plate Tectonics. Frontiers in Earth Science, 8: 326.

Hawkesworth C, Kemp A. 2006. Evolution of the continental crust. Nature. 443: 811 ~ 817.

Hayman P C, Thébaud N, Pawley M J, Barnes S J, Cas R A F, Amelin Y, Sapkota J, Squire R J, Campbell I H, Pegg I. 2015. Evolution of a ~2. 7 Ga large igneous province: A volcanological, geochemical and geochronological study of the Agnew Greenstone Belt, and new regional correlations for the Kalgoorlie Terrane (Yilgarn Craton, Western Australia). Precambrian Research, 270: 334 ~ 368.

Henri M, Tahar A, Fernando S, Miguel A S B. 2021. The Archean Pavas Block in Uruguay: Extension and tectonic evolution based on LA-ICP-MS U-Pb ages and airborne geophysics. Journal of South American Earth Sciences, 110: 103364.

Hildebrand R S, Whalen J B, Bowring S A. 2018. Resolving the crustal composition paradox by 3. 8 billion years of slab failure magmatism and collisional recycling of continental crust. Tectonophysics, 734: 69 ~ 88.

Hollis J A, Gool J A, Steenfel A, Garde A A. 2005. Greenstone belts in the central Godthåbsfjord region, southern West Greenland. GEUS Bulletin, 7: 65 ~ 68.

Jayananda M, Chardon D, Peucat J J, Tushipokla, Fanning C M. 2015. Paleo- to Mesoarchean TTG accretion and continental growth in the western Dharwar craton, Southern India: Constraints from SHRIMP U-Pb zircon geochronology, whole-rock geochemistry and Nd—Sr isotopes. Precambrian Research, 268: 295 ~ 322.

Jayananda M, Moyen J F, Martin H, Peucat J J, Auvray B, Mahabaleswar B. 2000. Late Archaean (2550~2520 Ma) juvenile magmatism in the Eastern Dharwar craton, southern India: constraints from geochronology, Nd—Sr isotopes and whole rock geochemistry. Precambrian Research, 99(3~4): 225 ~ 254.

Jayananda M. 2019. Geochronology and geochemistry of Meso- to Neoarchean magmatic epidote-bearing potassic granites, Western Dharwar Craton (Bellur—Nagamangala—Pandavpura corridor), Southern India: Implications for the successive stages of crustal reworking and cratonization. Geological Society London Special Publications, 486: 79 ~ 114.

Johnson I E, Kirkland C L, Gardiner N J, Brown M, Smithies R H, Santosh M. 2019. Secular change in TTG compositions: Implications for the evolution of Archaean geodynamics. Earth and Planetary Science Letters, 505: 65 ~ 75.

Juliani C, Fernandes C M D. 2010. Well-preserved Late Paleoproterozoic volcanic centers in the Sao Felix do Xingu region, Amazonian Craton, Brazil. Journal of Volcanology & Geothermal Research, 191(3~4): 167 ~ 179.

Kaur P, Zeh A, Chaudhri N, Dutta P. 2022. Detrital zircon U—Pb—Hf isotope record of conglomerates in the southern Aravalli orogen, NW India: Implications for stratigraphy, provenance and Archean to Paleoproterozoic crustal evolution. Precambrian Research, 379: 106800.

Kaur P, Zeh A, Chaudhri N. 2021. Archean to Proterozoic (3535~900 Ma) crustal evolution of the central Aravalli Banded Gneissic Complex, NW India: New constraints from zircon U—Pb—Hf isotopes and geochemistry. Precambrian Research, 359: 106179.

Keller C B, Harrison T M. 2020. Constraining crustal silica on ancient Earth. Proceedings of the National Academy of Sciences, 117(35): 202009431.

Khanna T C, Bizimis M, Yogodzinski G M, Mallick S. 2014. Hafnium—neodymium isotope systematics of the 2. 7 Ga Gadwal greenstone terrane, Eastern Dharwar craton, India: Implications for the evolution of the Archean depleted mantle. Geochimica et Cosmochimica Acta, 127: 10 ~ 24.

Khatun S, Mondal S K, Zhou MeiFu, Balaram V, Prichard H M. 2014. Prichard, Platinum-group element (PGE) geochemistry of Mesoarchean ultramafic—mafic cumulate rocks and chromitites from the Nuasahi Massif, Singhbhum Craton (India). Lithos, 205: 322 ~ 340.

Kinny P D, Wijbrans J R, Froude D O, Williams I S, Compston W. 1990. Age constraints on the geological evolution of the Narryer Gneiss Complex, Western Australia. Australian Journal of Earth Sciences, 37: 51 ~ 69.

Kirkland C L, Yakymchuk C, Gardiner N J, Szilas K, Hollis J, Olierook H, Steenfelt A. 2020. Titanite petrochronology linked to phase equilibrium modelling constrains tectono—thermal events in the Akia Terrane, West Greenland. Chemical Geology, 536: 119467.

Kirkland C L, Yakymchuk C, Szilas K, Evans N, Holli J, McDonald B, Gardiner N J. 2018. Apatite: a U-Pb thermochronometer or geochronometer? Lithos, 318: 143 ~ 157.

Kranendonk M J V, Smithies R H, Arthur H, Champion D C. 2007. Review: secular tectonic evolution of Archean continental crust: interplay between horizontal and vertical processes in the formation of the Pilbara Craton, Australia. Terra Nova, 19: 1 ~ 38.

Kranendonk M J V, Smithies R H, Hickman A H, Wingate M T D, Bodorkos S. 2010. Evidence for Mesoarchean (3. 2Ga) rifting of the Pilbara Craton: The missing link in an early Precambrian Wilson cycle. Precambrian Research, 177(1~2): 145 ~ 161.

Kröner A, Compston W. 1990. Archaean tonalitic gneiss of Finnish Lapland revisited: zircon ion-microprobe ages. Contributions to Mineralogy & Petrology, 104(3): 348 ~ 352.

Kröner A, Puustinen K, Hickman M. 1981. Geochronology of an archaean tonalitic gneiss dome in Northern Finland and its relation with an unusual overlying volcanic conglomerate and komatiitic greenstone. Contrib Mineral Petrol, 76: 33 ~ 41.

Lankvelt A V, Schneider D A, Biczok J, McFarlane C R M, Hattori K. 2016. Decoding Zircon Geochronology of Igneous and Alteration Events Based on Chemical and Microstructural Features: a Study from the Western Superior Province, Canada. Journal of Petrology, 57: 1309 ~ 1334.

Lauri L S, Andersen T, Hölttä P, Huhma H, Graham S. 2011. Evolution of the Archaean Karelian Province in the Fennoscandian Shield in the light of U-Pb zircon ages and Sm-Nd and Lu—Hf isotope systematics. Journal of the Geological Society, 168(1): 201 ~ 218.

Leal L R, Teixeira W, Cunha J C, Macambira M J. 1998. Arcahean tonalitic—trondhjemitic and granitic plutonism in the Gavião Block, São Francisco Craton, Bahia, Brazil: geochemical and geochronological characteristics. Brazilian Journal of Geology, 28: 209 ~ 220.

Li Dapeng, Chen Yuelong, Xue Guoliang, Kang Huang, Yu Yang, Geng Jianzheng, Zhang Yulong, Li Ting. 2020. Initiation of modern-style subduction in the Neoarchean: From plume to subduction with frequent slab break-off. Geological Society of America Bulletin, 132(9~10): 2119 ~ 2134.

Li Dengfeng, Hollings P, Chen Huayong, Sun Xiaoming, Tan Chuyan, Zurevinski S. 2020. Zircon U-Pb and Lu—Hf systematics of the major terranes of the Western Superior Craton, Canada: Mantle—

crust interaction and mechanism(s) of craton formation. Gondwana research: international geoscience journal, 78: 261 ~ 277.

Liu Jin, Zhang Jian, Liu Zenghong, Liu Xiaoguang, Cheng Changquan, Wang Zhigao, Zhao Chen, Yu Hongchao. 2022. Origin of the ca. 3.1 Ga Luanjiajie rock assemblage in the northeastern margin of the North China Craton: New constraints on the Mesoarchean geodynamic regime. Precambrian Research, 376: 106697.

Liu Shuwen, Wang Maojiang, Wan Yusheng, Guo Rongrong, Wang Wei, Wang Kang, Guo Boran, Fu Jinghao, Hu Fangyang. 2017. A reworked ~3.45Ga continental microblock of the North China Craton: Constraints from zircon U—Pb—Lu—Hf isotopic systematics of the Archean Beitai—Waitoushan migmatite—syenogranite complex. Precambrian Research, 303: 332 ~ 354.

Lobach-Zhuchenko S B, Ryborak M V, Saltykova T E, Sergeev S A, Lokhov K I, Bobrova E M, Sukach V V, Skublov S G, Berezhnaya N G, Al'bekov A Y. 2017. The Archean formation of the Sarmatian continental crust. Russian Geology and Geophysics, 58(12): 1494 ~ 1517.

Lopes L B L, Ganade C E, Campos L D, Rodrigues J, Oliveira L B T D, Larizzatti J H, Shen Mangting, Gao Tianshan, Xu Ming, Zhou Yan, Yao Zhongyou. 2021. Crustal reworking and Archean TTG generation in the south Gavião Block, São Francisco Craton, Brazil. Precambrian Research, 363(1~2): 106333.

Maibam B, Gerdes A, Goswami J N. 2016. U-Pb and Hf isotope records in detrital and magmatic zircon from eastern and western Dharwar craton, southern India: Evidence for coeval Archaean crustal evolution. Precambrian Research, 275: 496 ~ 512.

Maibam B, Maibam B, Goswami J N, Srinivasan R. 2011. Pb-Pb zircon ages of Archaean metasediments and gneisses from the Dharwar craton, southern India: Implications for the antiquity of the eastern Dharwar craton. Journal of Earth System Science, 120: 643 ~ 661.

Manikyamba C, Pahari A, Santosh M, Ray J, Sindhuja C S, Subramanyam K S V, Singh M R. 2020. Mesoarchean gabbro—anorthosite complex from Singhbhum Craton, India. Lithos, 366: 105541.

Mänttäri I, Hölttä P. 2002. U-Pb dating of zircons and monazites from Archean granulites in Varpaisjärvi, Central Finland:: Evidence for multiple metamorphism and Neoarchean terrane accretion. Precambrian Research, 118: 101 ~ 131.

Marimon R S, Hawkesworth C J, Dantas E L, Trouwa R A J, Teixeirad W, Hackspacher P C, Fetter A, Ávila C A, Volante S, Netoa A V C, Bongiolo E M, Vinagre R, Simon M. 2022. The generation and evolution of the Archean continental crust: The granitoid story in southeastern Brazil. Geoscience Frontiers, 13(4): 101402.

Martin H, Peucat J J, Sabaté P, Cunha J C. 1997. Crustal evolution in the early Archaean of South America: example of the Sete Voltas Massif, Bahia State, Brazil. Precambrian Research, 82(1~2): 35 ~ 62.

Masquelin H, Afa T, Scaglia F, Basei M A S. 2021. The Archean Pavas Block in Uruguay: Extension and tectonic evolution based on LA-ICP-MS U-Pb ages and airborne geophysics. Journal of South American Earth Sciences, 110: 103364.

Maya J M, Bhutani R, Balakrishnan S, Sandhya S R. 2017. Petrogenesis of 3.15 Ga old Banasandra komatiites from the Dharwar craton, India: Implications for early mantle heterogeneity. Geoscience Frontiers, 8(3): 467 ~ 481.

Medeiros E L M, Cruz S C P, Barbosa J S F, Paqiette J L, Peucat J J, Jesus S D S G P D, Barbosa R G, Brito R S C D, Carneiro M A. 2017. The Santa Izabel Complex, Gavião Block, Brazil: Components, geocronology, regional correlations and tectonic implications. Journal of South American Earth Sciences, 80: 66 ~ 94.

Mello E F, Xavier R P, McNaughton N J, Hagemann S G, Fletcher I, Snee L. 2006. Age constraints on felsic intrusions, metamorphism and gold mineralisation in the Palaeoproterozoic Rio Itapicuru greenstone belt, NE Bahia State, Brazil. Miner Deposita, 40: 849 ~ 866.

Melnyk M, Davis D W, Cruden A R, Stern R A. 2006. U-Pb ages constraining structural development of an Archean terrane boundary in the Lake of the Woods area, western Superior Province, Canada. Canadian Journal of Earth Sciences, 43(7): 967 ~ 993.

Meng Fanchao, Tian Yulu, Kerr A C, Wang Qianjun, Chen Yong, Zhou Yaoqi, Yang Fei. 2022. Neoarchean reworking of Mesoarchean and Paleoarchean crust (3.4~3.0Ga) within the North China Craton: Constraints from zircon U-Pb geochronology and Lu—Hf isotopes from the basement of the Bohai Bay Basin. Precambrian Research, 369: 106497.

Mikhalsky E V, Beliatsky B V, Sheraton J W, Roland N W. 2006. Two distinct Precambrian terranes in the Southern Prince Charles Mountains, East Antarctica: SHRIMP dating and geochemical constraints. Gondwana Research, 9(3): 291 ~ 309.

Mikhalsky E V, Henjes-Kunst F, Belyatsky B V, Roland N W, Sergeev S A. 2010. New Sm-Nd, Rb-Sr, U-Pb and Hf isotope systematics for the southern Prince Charles Mountains (East Antarctica) and its tectonic implications. Precambrian Research, 182: 101 ~ 123.

Mikkola P, Huhma H, Heilimo E, Whitehouse M. 2011. Archean crustal evolution of the Suomussalmi district as part of the Kianta Complex, Karelia: Constraints from geochemistry and isotopes of granitoids. Lithos, 125(1~2): 287 ~ 307.

Mishra S, Deomurari M P, Wiedenbeck M, Goswami J N, Ray S, Saha A K. 1999. $^{207}Pb/^{206}Pb$ zircon ages and the evolution of the Singhbhum Craton, eastern India: an ion microprobe study. Precambrian Research, 93: 139 ~ 151.

Misra S. 2006. Precambrian chronostratigraphic growth of Singhbhum—Orissa Craton, eastern Indian shield: an alternative model. Geol. Soc. India, 67: 356 ~ 378.

Monda S K, Ripley E M, Li Chusi, Frei R. 2006. The genesis of Archaean chromitites from the Nuasahi and Sukinda massifs in the Singhbhum Craton, India—ScienceDirect. Precambrian Research, 148(1~2): 45 ~ 66.

Monrad, J. R. 1983. Evolution of sialic terranes in the vicinity of the Holenarsipur belt, Hassan District, Karnataka, India. In Precambrian of South India, 4: 343 ~ 364.

Moreto C P N, Monteiro L V S, Xavier R P, Amaral W S, Santos T J D, Juliani C, Filho C R D S. 2011. Mesoarchean (3.0 and 2.86Ga) host rocks of the iron oxide—Cu—Au Bacaba deposit, Carajás Mineral Province: U-Pb geochronology and metallogenetic implications. Miner Deposita, 46: 789 ~ 811.

Moreto C P N, Monteiro L V S, Xavier R P, Creaser R A, DuFrane S A, Tassinari C C G, Sato K, Kemp A I S, Amaral W S. 2015a. Neoarchean and Paleoproterozoic Iron Oxide—Copper—Gold Events at the Sossego Deposit, Carajás Province, Brazil: Re-Os and U-Pb Geochronological Evidence. Economic Geology, 110(3): 809 ~ 835.

Moreto C P N, Monteiro L V S, Xavier R P, Creaser R A, DuFrane S A, Melo G H C, Silva M A D D, Tassinari C C G, Sato Kei. 2015b. Timing of multiple hydrothermal events in the iron oxide—copper—gold deposits of the Southern Copper Belt, Carajas Province, Brazi. Mineralium deposita, 50(5): 517 ~ 546.

Moser D E, Flowers R M, Hart R J. 2001. Birth of the Kaapvaal

Tectosphere 3.08 Billion Years Ago. Science, 291: 465 ~ 468.

Mouli C T, Arijit R, Kumar D G, Upadhyay D, Chakrabarti R. 2019. Evidence of crustal reworking in the Mesoarchean: Insights from geochemical, U-Pb zircon and Nd isotopic study of a 3.08~3.12 Ga ferro—potassic granite—gneiss from north-eastern margin of Singhbhum Craton, India. Lithos, 330~331: 16 ~ 34.

Moyen J F. 2011. The composite Archaean grey gneisses: Petrological significance, and evidence for a non-unique tectonic setting for Archaean crustal growth. Lithos, 123(1~4): 21 ~ 36.

Mueller P A, Shuster R D, Wooden J L, Erslev E A, Bowes D R. 1993. Age and composition of Archean crystalline rocks from the southern Madison Range, Montana: Implications for crustal evolution in the Wyoming craton. Geological Society of America Bulletin, 105: 437 ~ 446.

Mukherjee R, Mondal S K, Frei R, Rosing M T, Waight T E, Zhong Hong, Kumar G R R. 2012. The 3.1Ga Nuggihalli chromite deposits, Western Dharwar craton (India): Geochemical and isotopic constraints on mantle sources, crustal evolution and implications for supercontinent formation and ore mineralization. Lithos, 155: 392 ~ 409.

Næraa T, Scherstén A, Rosing M T, Kemp A I, Hoffmann J E, Kokfelt T F, Whitehouse M J. 2012. Hafnium isotope evidence for a transition in the dynamics of continental growth 3.2 Gyr ago. Nature, 485: 627 ~ 630.

Nagel T J, Hoffmann J E, Münker C. 2012. Generation of Eoarchean tonalite—trondhjemite—granodiorite series from thickened mafic arc crust. Geology, 40(4): 375 ~ 378.

Nance R D, Murphy J B, Santosh M. 2014. The supercontinent cycle: A retrospective essay. Gondwana Research, 25: 4 ~ 29.

Nandi A, Kumar T V, Babu E V S S K, Vadlamani R. 2023. Uranium—Pb ages of detrital zircon from the Mesoarchean Sukma and Neoarchean Bengpal supracrustal groups: Evidence forunconformable stratigraphic relations and implications forPrecambrian stratigraphy of the Bastar Craton, southcentral India. Journal of Asian Earth Sciences, 251: 105671.

Nelson D R, Bhattacharya H N, Thern E R, Altermann W. 2014. Geochemical and ion-microprobe U-Pb zircon constraints on the Archaean evolution of Singhbhum Craton, eastern India. Precambrian Research, 255: 412 ~ 432.

Nutman A P, Cordani U G. 1993. SHRIMP U-Pb zircon geochronology of Archaean granitoids from the Contendas—Mirante area of the São Francisco Craton, Bahia, Brazil. Precambrian Research, 63(3~4): 179 ~ 188.

Nutman A P, Friend C R L, Barker S L L, McGregor V R. 2004. Inventory and assessment of Palaeoarchaean gneiss terrains and detrital zircons in southern West Greenland. Precambrian Research, 135(4): 281 ~ 314.

Nutman A P,Wan Yusheng, Du Lilin, Friend C R L, Dong Chunyan, Xie Hangqiang, Wang Wei, Sun Huiyi, Liu Dunyi. 2011. Multistage late Neoarchaean crustal evolution of the North China Craton, eastern Hebei. Precambrian Research, 189(1~2): 43 ~ 65.

Olierook H K H, Kirkland C L, Hollis J A, Gardiner Ni J, Yakymchuk C, Szilas K, Hartnady M I H, Barham M, McDonald B J, Evans N J, Steenfelt A, Waterton P. 2021. Regional zircon U-Pb geochronology for the Maniitsoq region, southwest Greenland. Scientific Data, 8: 139.

Olierook H K H, Kirkland C L, Szilas K, Hollis J A, Gardiner N J, Steenfelt A, Qiang Jiang, Yakymchuk C, Evans N J, McDonald B J. 2020. Differentiating between Inherited and Autocrystic Zircon in Granitoids. Journal of Petrology, 61(8): 81.

Oliveira E P, Macnaughton N J, Zincone S, Talavera C. 2020. Birthplace of the São Francisco Craton, Brazil: Evidence from 3.60 to 3.64Ga Gneisses of the Mairi Gneiss Complex. Terra Nova, 32: 281 ~ 289.

Oliveira E P, Mcnaughton N J, Armstrong R. 2010. Mesoarchaean to Palaeoproterozoic growth of the northern segment of the Itabuna—Salvador—Curaca orogen, Sao Francisco craton, Brazil. Geological Society London Special Publications, 338(1): 263 ~ 286.

Oliveira E P, Mello E F, McNaughton N. 2002. Reconnaissance U-Pb geochronology of Precambrian quartzites from the Caldeirão belt and their basement, NE São Francisco Craton, Bahia, Brazil: implications for the early evolution of the Paleoproterozoic Itabuna—Salvador—Curaçá orogen. Journal of South American Earth Sciences, 15(3): 349 ~ 362.

Oliveira E P, Talavera C, Windley B F, Zhao Lei, Semprich J J, McNaughton N J, Amaral W S, Sombini G, Navarro M, Silva Dailto. 2019. Mesoarchaean (2820Ma) high-pressure mafic granulite at Uauá, So Francisco Craton, Brazil, and its potential significance for the assembly of Archaean supercratons. Precambrian Research, 331: 105366.

Ordóñez-Calderón J C, Polat A, Fryer B J, Gagnon J E, Raith J G, Appel P W U. 2008. Evidence for HFSE and REE mobility during calc—silicate metasomatism, Mesoarchean (3075Ma) Ivisaartoq greenstone belt, southern West Greenland. Precambrian Research, 161(3~4): 317 ~ 340.

Palin R M, White R W, Green E C R. 2016. Partial melting of metabasic rocks and the generation of tonalitic—trondhjemitic—granodioritic(TTG) crust in the Archaean: Constraints from phase equilibrium modelling. Precambrian Research, 287: 73 ~ 90.

Paquette J L, Ionov D A, Agashev A M, Gannoun A, Nikolenko E I. 2017. Age, provenance and Precambrian evolution of the Anabar shield from U-Pb and Lu—Hf isotope data on detrital zircons, and the history of the northern and central Siberian craton. Precambrian Research, 301: 134 ~ 144.

Peucat J J, Mascarenhas J F, Barbosa J S F, Souza S L D, Marinho M M M, Fanning C M, Leite C M M. 2002. 3.3 Ga SHRIMP U-Pb zircon age of a felsic metavolcanic rock from the Mundo Novo greenstone belt in the São Francisco craton, Bahia (NE Brazil). Journal of South American Earth Sciences, 15(3): 363 ~ 373.

Pidgeon R T, Macambira M J B, Lafon J. 2000. Th—U—Pb isotopic systems and internal structures of complex zircons from an enderbite from the Pium Complex, Carajas Province, Brazil; evidence for the ages of granulite facies metamorphism and the protolith of the enderbite. Chemical Geology, 166(1): 159 ~ 171.

Polat A, Longstaffe F, Weisener C, Fryer B, Frei R, Kerrich R. 2012. Extreme element mobility during transformation of Neoarchean (ca. 2.7Ga) pillow basalts to a Paleoproterozoic (ca. 1.9Ga) paleosol, Schreiber Beach, Ontario, Canada. Chemical Geology, 326: 145 ~ 173.

Polat A, Wang L, Appel P W U. 2015. A review of structural patterns and melting processes in the Archean craton of West Greenland: Evidence for crustal growth at convergent plate margins as opposed to non-uniformitarian model. Tectonophysics, 662: 67 ~ 94.

Qiu Xiaofei, Chen Weixiong, Xu Daliang, Zhao Xiaoming, Dong Xirun. 2022&. Crustal evolution in Archean for the Kongling Complex in the Yangtze Craton Nucleus. South China Geology, 38(1): 56 ~ 66.

Qiu Xiaofei, Zhao Xiaoming, Yang Hongmei, Lu Shansong, Wu Nianwen, Jiang Tuo, Gu Tao, Wang Yunfeng. 2018a. Geochemical and Nd isotopic compositions of the Palaeoproterozoic metasedimentary rocks in the Kongling complex, nucleus of Yangtze craton, South China block: implications for provenance and tectonic evolution. Geological Magazine, 155(6): 1263 ~ 1276.

Qiu Xiaofei, Ling Wenli., Liu Xiaoming, Lu Shansong, Jiang Tuo, Wei Yunxu, Peng Lianhong, Tan Juanjuan. 2018b. Evolution of the Archean continental crust in the nucleus of the Yangtze block: Evidence from geochemistry of 3.0 Ga TTG gneisses in the Kongling high-grade metamorphic terrane, South China. Journal of Asian Earth Sciences, 154: 149 ~ 161.

Ranjan S, Upadhyay D, Abhinay K, Srikantappa C. 2020. Paleoarchean and Neoarchean Tonalite—Trondhjemite—Granodiorite (TTG) and granite magmatism in the Western Dharwar Craton, southern India: Implications for Archean continental growth and geodynamics. Precambrian Research, 340: 105630.

Ratheesh-Kumar R T, Santosh M, Yang QiongYan, Ishwar-Kumar C, Chen NengSong, Sajeev K. 2016. Archean tectonics and crustal evolution of the Biligiri Rangan Block, southern India. Precambrian Research, 275: 406 ~ 428.

Ravindran A, Mezger K, Balakrishnan S, Berndt J, Ranjan S, Upadhyay D. 2023. Formation of Paleo- to Meso-Archean continental crust in the western Dharwar Craton, India: Constraints from UPb zircon ages and Hf—Pb—Sr isotopes of granitoids and sedimentary rocks. Chemical Geology, 615: 121196.

Rosen O M, Levskii LK, Zhuravlev D Z, Rotman A Y, Spetsius Z V, Zinchuk N N, Manakov A V, Serenko V P. 2006. Paleoproterozoic accretion in the Northeast Siberian craton: Isotopic dating of the Anabar collision system. Stratigraphy & Geological Correlation, 14 (6): 581 ~ 601.

Rosing M T, Nutman A P, Løfqvist L. 2001. A new fragment of the early earth crust: the Aasivik terrane of West Greenland. Precambrian Research, 105(2~4): 115 ~ 128.

Sameer R, Upadhyay D, Abhinay K. 2020. Paleoarchean and Neoarchean Tonalite—Trondhjemite— Granodiorite (TTG) and granite magmatism in the Western Dharwar Craton, southern India: Implications for Archean continental growth and geodynamics. Precambrian Research, 340: 105630.

Santosh M Y, Yang Qiangyan, Shaji E, Mohan M R, Tsunogae T, Satyanarayanan M. 2016. Oldest rocks from Peninsular India: Evidence for Hadean to Neoarchean crustal evolution. Gondwana research: international geoscience journal, 29(1): 105 ~ 135.

Santos-Pinto M, Peucat J J, Martin H, Barbosa J S F, Fanning C M, Cocherie A, Paquette JL. 2012. Crustal evolution between 2.0 and 3.5 Ga in the southern Gavião block (Umburanas—Brumado—Aracatu region), São Francisco Craton, Brazil: A 3.5~3.8 Ga proto-crust in the Gavião block? Journal of South American Earth Sciences, 40: 129 ~ 142.

Sarma D S, McNaughton N J, Belusova E, Mohan M R, Fletcher I R. 2012. Detrital zircon U-Pb ages and Hf-isotope systematics from the Gadag Greenstone Belt: Archean crustal growth in the western Dharwar Craton, India. Gondwana Research, 22(3~4): 843 ~ 854.

Sato K, Siga O, Nutman A P, Basei Mi A S, McReath I, Kaulfuss G. 2003. The Atuba Complex, Southern South American Platform: Archean Components and Paleoproterozoic to Neoproterozoic Tectonothermal Events. Gondwana Research, 6(2): 251 ~ 263.

Savko K, Alexander S, Alexander L. 2019. Mesoarchean Silicic Volcanics in the Kursk Block of the Voronezh Crystalline Massif: Composition, Age, and Correlations with the Ukrainian Shield. Doklady Earth Sciences, 486: 719 ~ 723.

Schersten A, Garde A A. 2013. Complete hydrothermal re-equilibration of zircon in the Maniitsoq structure, West Greenland: A 3001 Ma minimumage of impact? Meteoritics and Planetary Science, 48(8): 1472 ~ 1498.

Schmitz M D, Bowring S A, Southwick D L, Boerboom T J, Wirth K R. 2006. High-precision U-Pb geochronology in the Minnesota River Valley Subprovince and its bearing on Neoarchean to Paleoproterozoic evolution of the Southern Superior Province. Geological Society of America Bulletin, 110: 82 ~ 93.

Schofield D I, Thomas R J, Goodenough K M, Waele B D, Pitfield P E J, Key R M, Bauer W, Walsh G J, Lidke D J, Ralison A V, Rabarimanana M, Rafahatelo J M, Randriamananjara T. 2010. Geological evolution of the Antongil Craton, NE Madagascar. Precambrian Research, 182(3): 187 ~ 203.

Sergeev S A, Bibikova E V, Matukov D I, Lobach-Zhuchenko S B. 2007. Age of the magmatic and metamorphic processes in the vodlozero complex, Baltic shield: An ion microprobe (SHRIMP II) U—Th—Pb isotopic study of zircons. Geochemistry International, 45(2): 198 ~ 205.

Sergeev S A, Lobach-Zhuchenko S B, Arestova N A, Tolmacheva E V, Berezhnaya N G, Matukov D I, Lokhov K I, Antonov A V. 2008. Age and geochemistry of zircons from the ancient granitoids of the Vyg River, Southeastern Karelia. Geochemistry International, 46 (6): 595 ~ 607.

Shatsky V S, Ragozin A., Wang Qin, Wu Meiqian. 2022. Evidence of Eoarchean crust beneath the Yakutian kimberlite province in the Siberian craton. Precambrian Research, 369: 106512.

Sheraton J W, Tingey R J, Black L P, Offe L A, Ellis D J. 1987. Geology of an unusual Precambrian high-grade metamorphic terrane—Enderby Land and western Kemp Land, Antarctica. Geology, 223: 47 ~ 51.

Shirey S B, Richardson S H. 2011. Start of the Wilson Cycle at 3 Ga Shown by Diamonds from Subcontinental Mantle. Science, 333: 434 ~ 436.

Sindhuja C S, Pahari A, Manikyamb C, Santosh M, Li Tang, Ray J, Subramanyam K S V, Paul M, Gonzalez-Alvarez I, Sruthi P C. 2022. Crustal stabilization: Evidence from the geochemistry and U-Pb detrital zircon geochronology of quartzites from Simlipal Complex, Singhbhum Craton, India. Geoscience Frontiers, 13(1): 46 ~ 61.

Smithies R H, Champion D C, Cassidy K F. 2003. Formation of Earth's early Archaean continental crust. Precambrian Research, 127: 89 ~ 101.

Smithies R H, Champion D C, Kranendonk M J V. 2009. Formation of Paleoarchean continental crust through infracrustal melting of enriched basalt. Earth and Planetary Science Letters, 281: 298 ~ 306.

Smithies R H, Champion D C, Kranendonk M J V, Howard H M, Hickman A H. 2005. Modern-style subduction processes in the Mesoarchaean: Geochemical evidence from the 3.12 Ga Whundo intra-oceanic arc. Earth and Planetary Science Letters, 231: 221 ~ 237.

Song Biao, Nutman A P, Liu Dunyi, Wu Jiashan. 1996. 3800 to 2500 Ma crustal evolution in the Anshan area of Liaoning Province, northeastern China. Precambrian Research, 78: 79 ~ 94.

Steenfelt A, Hollis J A, Kirkland C L, Sandrin A, Gardiner N J, Olierook H K H, Szilas K, Waterton P, Yakymchuk C. 2020. The Mesoarchaean Akia terrane, West Greenland, revisited: New insights based on spatial integration of geophysics, field observation, geochemistry and geochronology. Precambrian Research, 352: 105958.

Strong J W D, Cruden A R, Cawood P A, Davis D W. 2022. Eo-Paleoarchean detrital zircon in the Winnipeg River terrane, Western Superior Province: Provenance and implications. Precambrian Research, 379: 106802.

Suhr N, Hoffmann J E, Kroener A, Schröder S. 2014. Archaean granulite-facies paragneisses from central Swaziland: Inferences on Palaeoarchaean crustal reworking and a complex metamorphic history. Journal of the Geological Society, 172(1): 139 ~ 152.

Sukach V V. 2014. Mesoarchean greenstone structures of the Middle Dnipro area of the Ukrainian shield: Stratigraphic sections, substance composition and age correlation. Mineralogicheskii Zhurnal, 36 (2): 77 ~ 91.

Sun Huiyi, Xie Hangqaing, Liu Shouji, Dong Chunyan, Liu Dunyi, Wan Yusheng. 2016&. Archean magmatism and metamorphism in the Huangbaiyu—Yangyashan area, eastern Hebei Province: Evidence from SHRIMP zircon U-Pb dating. Geological Bulletin of China, 35(1): 27 ~ 42.

Sun McDonough W F. 1989. Chemical and isotopic systematics of oceanic basalts: Implications for mantle composition and processes. Geological Society, London, Special Publications, 42: 313 ~ 345.

Sylvester P J, Cambel, Bowyer D A. 1997. Niobium/uranium evidence for early formation of the continental crust. Science, 275: 521 ~ 523.

Szilas K, Tusch J, Hoffmann J H, Garde A A, Münker C. 2017. Hafnium isotope constraints on the origin of Mesoarchaean andesites in southern West Greenland, North Atlantic Craton. Geological Society, London, Special Publications, 449: 19 ~ 38.

Szilas K, Kelemen P B, Bernstein S. 2015. Peridotite enclaves hosted by Mesoarchaean TTG-suite orthogneisses in the Fiskefjord region of southern West Greenland. GeoResJ, 7: 22 ~ 34.

Tang Ming, Lee C A, Rudnick R L, Condie K C. 2020. Rapid mantle convection drove massive crustal thickening in the late Archean. Geochimica et Cosmochimica Acta, 278: 6 ~ 15.

Tang Yanjie, Zhang Hongfu, Ying Jifeng, Su Benxun. 2013. Widespread refertilization of cratonic and circum-cratonic lithospheric mantle. Earth-Science Reviews, 118: 45 ~ 68.

Taylor J, Stevens G, Buick I S, Lana C. 2012. Successive midcrustal, high-grade metamorphic events provide insight into Mid-Archean mountain-building along the SE margin of the proto-Kaapvaal craton. Geological Society of America Bulletin, 124(7~8): 1191 ~ 1211.

Taylor J, Stevens G. 2019. Comment on "High-temperature metamorphism and crustal melting at ca. 3. 2 Ga in the eastern Kaapvaal craton, southern Africa" by Kröner et al. ——why heating of the Ancient Gneiss Complex by a mantle plume at 3. 2 Ga is not a viable tectonic model. Precambrian Research, 332: 105307.

Taylor P N, Chadwick B, Moorbath S, Ramakrishnan M, Viswanatha M N. 1984. Petrography, chemistry and isotopic ages of Peninsular Gneiss, Dharwar acid volcanic rocks and the Chitradurga granite with special reference to the late Archean evolution of the Karnataka craton, southern India. Precambrian Research, 23(3~4): 349 ~ 375.

Taylor S R, Mclennan S M. 1995. The geochemical evolution of the continental crust. Rev. Geophys, 33: 241 ~ 265.

Tchemeni R, Pouclet A, Mezger K, Nsifa N E, Vicat J. 2004. Single zircon Pb-Pb and Sm-Nd whole rock ages for the Ebolowa greenstone belts: Evidence for pre-2. 9 Ga terranes in the Ntem Complex (South Cameroon). Journal of the Cameroon academy of sciences, 4: 235 ~ 246.

Tomlinson K Y, Stott G M, Percival J A, Stone D. 2004. Basement terrane correlations and crustal recycling in the western Superior Province: Nd isotopic character of granitoid and felsic volcanic rocks in the Wabigoon subprovince, N. Ontario, Canada. Precambrian Research, 132(3): 245 ~ 274.

Tucker R D, Ashwal L D, Handke M J, Hamilton M, Grange M, Rambeloson R A. 1999. U-Pb Geochronology and Isotope Geochemistry of the Archean and Proterozoic Rocks of North—Central Madagascar. The Journal of Geology, 107: 135 ~ 153.

Upadhyay D, Chattopadhyay S, Mezger K. 2019. Formation of Paleoarchean—Mesoarchean Na-rich (TTG) and K-rich granitoid crust of the Singhbhum craton, eastern India: Constraints from major and trace element geochemistry and Sr—Nd—Hf isotope composition. Precambrian Research, 327: 255 ~ 272.

Waele B D, Lacorde M, Vergara F, Chan G. 2015. New insights on proterozoic tectonics and sedimentation along the peri-Gondwanan West African margin based on zircon U-Pb SHRIMP geochronology. Precambrian Research, 259: 156 ~ 175.

Wan Yusheng, Dong Chunyan, Xie Hangqiang, Li Yuan, Wang Yuqing, Wang Kunli. 2022&. Huge growth of the late Mesoarchean—early Neoarchean (2. 6 ~ 3. 0 Ga) continental crust in the North China Craton: A review. Journal of Geomechanics, 28(5): 866 ~ 906

Wan Yusheng, Liu Dunyi, Nutman A, Zhou Hongying, Dong Chunyan, Yin Xiaoyan, Ma Mingzhu. 2012. Multiple 3. 8 ~ 3. 1Ga tectono—magmatic events in a newly discovered area of ancient rocks (the Shengousi Complex), Anshan, North China Craton. Journal of Asian Earth Sciences, 54~55: 18 ~ 30.

Wan Yusheng, Liu Dunyi, Song Biao, Wu Jishan, Yang Chonghui, Zhang Zongqing, Geng Yuansheng. 2005. Geochemical and Nd isotopic compositions of 3. 8 Ga meta-quartz dioritic and trondhjemitic rocks from the Anshan area and their geological significance. Journal of Asian Earth Sciences, 24(5): 563 ~ 575.

Wan Yusheng, Song Biao, Liu Dunyi, Li Huimin, Yang Chun, Zhang Qiaoda, Yang Chonghui, Geng Yuansheng, Shen Qihan. 2001&. Institute of Geology, Chinese Academy of Geological Sciences, Beijing,) Open Laboratory on Isotope Geology, Ministry of Land, Resource of P R. 2001. Geochronology and Geochemistry of 3. 8 ~ 2. 5 Ga Ancient Rock Belt in the Dongshan Scenic Park, Anshan Area. Acta Geologica Sinica, 75(3): 363 ~ 370.

Wan Yusheng, Xie Hangqiang, Wang Huichu, Li Pengchuan, Chu Hang, Xiao Zhibin, Dong Chunyan, Liu Shouji, Li Yuan, Hao Guangming, Liu Dunyi. 2021&. Discovery of ~3. 8 Ga TTG rocks in eastern Hebei, North China Craton. Acta Geologica Sinica, 95 (5): 1321 ~ 1333.

Wan Yusheng, Liu Dunyi, Nutman A, Zhou Hongying, Dong Chunyan, Yin Xiaoyan, Ma Mingzhu. 2012. Multiple 3. 8 ~ 3. 1Ga tectono—magmatic events in a newly discovered area of ancient rocks (the Shengousi Complex), Anshan, North China Craton. Journal of Asian Earth Sciences, 54~55: 18 ~ 30.

Wang DeYing, Wang QingBin, Liu XiaoJian, Zhao Meng, Hao YiWei. 2019&. Characteristics and developing patterns of gneiss buried hill weathering crust reservoir in the sea area of the Bohai Bay basin. Acta Petrologica Sinica, 35(4): 1181 ~ 1193.

Wang YaFei, Li XianHua, Jin Wei, Zeng Lingsen, Zhang JiaHui. 2020. Generation and maturation of Mesoarchean continental crust in the Anshan Complex, North China Craton. Precambrian Research, 341: 105651.

Wang YaFei, Li XianHua, Jin Wei, Zhang JiaHui. 2015. Eoarchean ultra-depleted mantle domains inferred from ca. 3. 81Ga Anshan trondhjemitic gneisses, North China Craton. Precambrian Research, 263: 88 ~ 107.

Waterton P, Hyde W R, Tusch J, Hollis J A, Kirkland C L, Kiney C,

Yakymchuk C, Gardiner N J, Zakharov D, Olierook H K H, Lightfoot P C, Szilas K. 2020. Geodynamic Implications of Synchronous Norite and TTG Formation in the 3Ga Maniitsoq Norite Belt, West Greenland. Frontiers in Earth Science, 8: 562062.
Westraat J, Kisters A M, Poujol M, Stevens G. 2005. Transcurrent shearing, granite sheeting and the incremental construction of the tabular 3.1 Ga Mpuluzi batholith, Barberton granite—greenstone terrane, South Africa. Journal of the Geological Society, 162(2): 373 ~ 388.
Windley B F, Kusky T, Polat A. 2021. Onset of plate tectonics by the Eoarchean. Precambrian Research, 352: 105980.
Wu Fuyuan, Zhang Yanbin, Yang Jinhui, Xie Liewen, Yang Yueheng. 2008. Zircon U-Pb and Hf isotopic constraints on the Early Archean crustal evolution in Anshan of the North China Craton. Precambrian Research, 167(3~4): 339 ~ 362.
Xu Nan, Wu Cailai, Zhao Miaomiao, Liu Chang. 2023&. Petrogenesis of Mangya diorites and its implication to tectonic evolution. Geological Review, 69(6): 2085 ~ 2111.
Yakymchuk C, Kirkland C L, Hollis J A, Kendricka J, Gardinerd N J, Szilasf K. 2020. Mesoarchean partial melting of mafic crust and tonalite production during high-T—low-P stagnant tectonism, Akia Terrane, West Greenland. Precambrian Research, 339: 105615.
Yang Chengxue, Santosh M, Lloyd J C, Glorie, Gao Pin, Bing Yu, Anilkumar Y, Anoop K S, Sung W K. 2023. The Coorg Block, southern India: Insights from felsic and mafic magmatic suites on Mesoarchean plate tectonics and correlation with supercontinent Ur. Gondwana Research, 118: 1 ~ 36.
Yang Qiongyan, Santosh M, Ganguly S, Arun-Gokul J, Dev S G D, Tsunogae T, Shaji E, Dong Yunpeng, Manikyamba C. 2016. Melt—fluid infiltration in Archean suprasubduction zone mantle wedge: Evidence from geochemistry, zircon U-Pb geochronology and Lu—Hf isotopes from Wynad, southern India. Precambrian Research, 281: 101 ~ 127.
Yu Bing, Santosh M, Amaldev T, Jang Yirang, Yang Chengxue. 2022. Paleo—Mesoarchean crustal evolution in the Coorg Block, southern India: Insights from magmatic and metamorphic records in mafic granulites. Precambrian Research, 370: 106537.
Yu Bing, Santosh M, Amaldev T, Palin R M. 2021. Mesoarchean (ultra)-high temperature and high-pressure metamorphism along a microblock suture: Evidence from Earth ′soldest khondalites in southern India. Gondwana research: international geoscience journal, 91(1): 129 ~ 151.
Yu Yang, Li Dapeng, Chen Yuelong, Sun Jian, Geng Jianzheng, Yang Fan, Han Yubing. 2022. Mesoarchean trondhjemitic continental nucleus and pre-plate tectonic crustal—mantle interactions of the Western Shandong Complex, North China Craton. Precambrian Research, 369: 106517.
Zhai Mingguo, Santosh M. 2011. The early Precambrian odyssey of the North China Craton: A synoptic overview. Gondwana Research, 20: 6 ~ 25.
Zhang Chuanlin, Zou Haibo, Li Huaikun, Wang Hongyan. 2013. Tectonic framework and evolution of the Tarim Block in NW China. Gondwana Research, 23: 1306 ~ 1315.
Zhang Jinpeng, Wang Yang. 2024&. An evaluation on the petrochemical diagrams for discriminating plagioclase- rich granitoids. Geological Review, 70(5): 1963 ~ 1980.
Zhang Qi, Yuan Jie. 2024&. The crisis and opportunity of geochemical research. Geological Review, 70(5): 1907 ~ 1926.
Zhang Shaobing, Zheng Yongfei, Wu Yuanbao, Zhao Zifu, Gao Shan, Wu Fuyuan. 2006. Zircon U-Pb age and Hf isotope evidence for 3.8 Ga crustal remnant and episodic reworking of Archean crust in South China. Earth and Planetary Science Letters, 252(1~2): 56 ~ 71.
Zhang Shihong, Wang Hongzhen. 2002&. A Perspective of Paleocontinental Reconstruction. Geological Review, 48(2): 198 ~ 213.
Zhang Shuanhong, Zhao Yue, Pei Junling, WangG Hongyu, Hu Guohui, Zhang Qiqi, Cai Yuhang, Kong Linghao, Wang Sen, Wang Kai. 2022&. A review on large igneous provinces (LIPs) and their implications for paleogeographic reconstruction and continental breakup. Geological Review, 68(5): 1634 ~ 1652.
Zhao Yan, DiWu Chunrong, Ao Wenhao, Wang Hongliang, Zhu Tao, Sun Yong. 2015&. Ca. 3.06 Ga granodioritic gneiss in Dunhuang block. Chinese Science Bulletin, 60(1):75 ~ 87.
Zheng Jianping, Griffin W L, O" Reilly S Y, Zhao Junhong, Wu Yuanbao, Liu G L, Pearson N, Zhang M, Ma C Q, Zheng Jianping, Griffin W, Reilly S O, Zhao J, Wu Y, Liu G, Pearson N, Zhang Ming, Ma Changqian, Zhang Zejun, Yu Chunmei, Su Yuping, Tang Huayun. 2009. Neoarchean (2.7~2.8Ga) accretion beneath the North China Craton: U-Pb age, trace elements and Hf isotopes of zircons in diamondiferous kimberlites. Lithos, 112(3~4): 188 ~ 202.
Zhou Hongying, Liu Dunyi, Wan Yusheng, Wilde S A, Wu Jiashan. 2007&. 3.3 Ga magmatic events in the Anshan area: new SHRIMP age and geochemical constraints. Acta Petrologica et Mineralogica, 26(2): 123 ~ 129.
Zhou Hongying, Liu Dunyi, Wan Yusheng. 2008&. 3.3 ~ 3.1 Ga magmatism in the Dongshan Complex, Anshan area, Liaoning, China: Evidence from SHRIMP U-Pb zircon dating. Geological Bulletin of China, 27(12): 2122 ~ 2126.

~3.1 Ga Global magmatic events and crustal evolution

BIAN Tianyi[1)], MENG Fanchao[1,2,3)], YANG Fei[1)]

1) *State Key Laboratory of Deep Oil and Gas, China University of Petroleum (East China), Qingdao, Shandong*, 266580;

2) *Laboratory for Marine Mineral Resources, Qingdao Marine Science and Technology Center, Qingdao, Shandong*, 266237

3) *Laoshan National Laboratory, Qingdao, Shandong*, 266061

Objectives: During the Archean, approximately 90% of the global craton′s crust may have formed, particularly during the 3.5~3.1 Ga, 2.8~2.7 Ga, and 2.6~2.5 Ga. More rocks are preserved from the 2.8~2.7 Ga and late 2.6~2.5 Ga periods. While the mechanisms of crustal accretion and remodeling are frequently investigated, research is limited by the scarcity of samples, resulting in relatively weak studies on magmatic events and crustal formation prior to 3.0 Ga. Furthermore, the understanding of earlier Preambrian magmatic events and crustal accretion remains controversial.

Methods: Building upon previous research, this study summarizes and compares zircon ages, rock types, whole-rock geochemistry, and zircon Lu—Hf—O isotope signatures of global Mesoproterozoic rocks, primarily from the 3.2~3.0 Ga period, in order to concluding the global magmatic events and crustal evolution patterns around 3.1 Ga.

Results: Rocks from the 3.2~3.0 Ga period are found across all continents, with a predominant concentration in the Northern Hemisphere, while the Southern Hemisphere exhibits a relatively smaller number in present. The peak zircon ages of these rocks are concentrated around 3.05 Ga and 3.15 Ga. The main lithologies include stromatolitic and peraluminous aeolian granite. The primary lithologies of the rocks consist of angstromatolite and aeolian granite with peraluminous characteristics. Different regions exhibit distinct rock assemblages, and the $\varepsilon_{Hf}(t)$ values of zircons from these regions demonstrate significant variations, reflecting differences in the origin and evolutionary history of the rocks. Most zircons have $\delta^{18}O$ values in equilibrium with mantle melt; however, some zircons exhibit higher $\delta^{18}O$ values, reaching +8.93‰, suggesting that the rock source areas underwent low-temperature alteration or mixing with crustal materials. The rocks display a right-tilted pattern characterized by an enrichment of light rare earth elements and a deficit of heavy rare earth elements, with pronounced europium anomalies. Overall, elements such as Th, U, K, and Pb are relatively enriched, whereas elements like Nb, Ta, P, Sm, and Ti are comparatively deficient.

Conclusions: The ~3.1 Ga rocks likely formed through partial melting of a basaltic source region that experienced low-temperature alteration. This source region originated from partial melting of a mildly deficient mantle around ~3.3 Ga. A global event of magmatism and crustal growth occurred during the early Mesoarchean (primarily between 3.2 and 3.0 Ga), with peaks at approximately 3.05 Ga and 3.15 Ga. Furthermore, tectonic regimes akin to modern plate motions began to emerge in certain areas during the Mesoarchean.

Keywords: Petrogenesis; Mesoarchean crustal growth; Magmatic event; TTG rocks

Acknowledgemengts: This study was supported by the Natural Science Foundation of China (No. 42272225), Science and Technology Innovation Foundation by Laoshan Laboratory, Natural Science Foundation of Shandong Province (No. ZR2021MD083) and Fundamental Research Funds for the Central Universities of Ministry of Education of China (No. 23CX09004A)

First author: Bian Tianyi, male, master student. Email: 1390485955@qq.com

Corresponding author: Meng Fanchao, male, professor, mainly working on teaching and research in Petrology and Geochemistry. Email: mengfc@upc.edu.cn

Manuscript received on: 2024-10-21; Accepted on: 2024-12-09; Published online on: 2024-12-20

Doi: 10.16509/j.georeview.2024.12.065 **Edited by**: ZHANG Yuxu

附表：全球克拉通中 3.1 Ga 左右时期的岩浆锆石和碎屑锆石分布表

Appendix table: Distribution table of magmatic and clastic zircons with ages about 3.1 Ga in the global cratons

样品号	岩性	采样地点	分析方法	原岩年龄(Ma)	±1σ	资料来源
华北克拉通						
05FW029	花岗岩	陈台沟	SHRIMP	3119		Wu Fuyuan et al.,2008
05FW033	奥长花岗岩	白家坟	SHRIMP	3140	31	Wu Fuyuan et al.,2008
01FW306	奥长花岗岩	白家坟	SHRIMP	3157	10	Wu Fuyuan et al.,2008
A0912	片麻状奥长花岗岩	东山杂岩西段	SHRIMP	3139	7	董春艳等,2013
A0504	细粒奥长花岗岩	东山杂岩带东端	SHRIMP II	3141	8	周红英等,2008

样品号	岩性	采样地点	分析方法	原岩年龄（Ma）	±1σ	资料来源
A0505	二长花岗岩	东山杂岩带东端	SHRIMP II	3142	5	周红英等,2008
A9604	石英闪长岩	东山杂岩带东端	SHRIMP II	3007	22	周红英等,2007
A9203	非均质花岗岩	立山	SHRIMP	3142	7	Song Biao et al.（1996）
Ch16	花岗岩	西鞍山矿区	SHRIMP	3001	8	Song Biao et al.，1996
A0513	二长花岗岩	深沟寺杂岩	SHRIMP II	3129	6	Wan Yusheng et. al.，2012
A9605	二长花岗岩	东山风景区	SHRIMP	3104	67	万渝生等,2001
DGS-12	绿泥石英片岩	大孤山	SHRIMP	3105	18	Dai Yanpei et al.，2014
DDGS-3	绿泥石英片岩	大孤山	LA-ICP-MS	3101	28	Dai Yanpei et al.，2014
DGS-14	混合片麻岩	大孤山	SIMS	3089	33	Dai Yanpei et al.，2014
C209-4	奥长花岗岩	锅底山	SIMS	3131	11	Wang Yafei et al.，2015
C209-6	奥长花岗岩	锅底山	SIMS	3136	20	Wang Yafei et al.，2015
A1117	片麻状正长花岗岩	铁架山	SHRIMP	3024	10	Dong Chunyan et al.，2017
C201-3	奥长花岗质片麻岩	丁山	SIMS	3144	6	Wang Yafei et al.，2020
17LSW01-1	二长花岗质片麻岩	东鞍山	LA-ICP-MS	3014	5	Bao Han et al.，2020
17LSW27-1	奥长花岗质片麻岩	金家岭	LA-ICP-MS	3012	13	Bao Han et al.，2020
C405-3	奥长花岗质片麻岩	深沟寺杂岩	SIMS	3135	5	Wang Yafei et al.，2020
C030-1	奥长花岗质片麻岩	立山	SIMS	3135	14	Wang Yafei et al.，2020
C345-1	二长花岗质片麻岩	陈台沟	SIMS	3144	2	Wang Yafei et al.，2020
C130-2	花岗片麻岩	陈台沟	SIMS	3136	9	Wang Yafei et al.，2020
C459-1	奥长花岗质片麻岩	立山	SIMS	3141	7	Wang Yafei et al.，2020
C455-1	奥长花岗质片麻岩	东山	SIMS	3135	13	Wang Yafei et al.，2020
C229-1	奥长花岗质片麻岩	锅底山	SIMS	3140	9	Wang Yafei et al.，2020
C303-2	奥长花岗质片麻岩	锅底山	SIMS	3136	8	Wang Yafei et al.，2020
C317-6	奥长花岗质片麻岩	营城子	SIMS	3145	7	Wang Yafei et al.，2020
C366-1	奥长花岗质片麻岩	营城子	SIMS	3138	5	Wang Yafei et al.，2020
C075-2	二长花岗质片麻岩	陈台沟	SIMS	3136	9	Wang Yafei et al.，2020
C345-2	二长花岗质片麻岩	陈台沟	SIMS	3140	3	Wang Yafei et al.，2020
J1111	片麻状二长花岗岩	冀东黄柏峪村北	SHRIMP	3107	20	孙会一等,2016
CHG14-2	TTGs	济阳坳陷	SHRIMP	3131	23	Meng Fanchao et. al.. 2022
CHG12-2	TTGs	济阳坳陷	LA-ICP-MS	3123	25	Meng Fanchao et. al.. 2022
CH917-3	表壳岩	济阳坳陷	LA-ICP-MS	3081	19	Meng Fanchao et. al.. 2022
CFD12-6-1-18	片麻岩	BBBCFD12-6-1 井	LA-ICP-MS	3166		王德英等,2019
J08/04	石英岩	曹庄	SHRIMP	3142	14	Allen et. al.. 2011
19LJ01-11	TTG 片麻岩	栾家界	SHRIMP	3115	49	Liu Jin et. al.. 2022
19LJ03-6	TTG 片麻岩	栾家界	SHRIMP	3092	96	Liu Jin et. al.. 2022
19LJ03-4	角闪岩	栾家界	SHRIMP	3105	89	Liu Jin et. al.. 2022
	铬云母石英岩	弓长岭二矿区东南	锆石离子探针	3186	5	万渝生等,1993
15Q22-2	花岗闪长质片麻岩	栾家界	LA-ICP-MS	3005	37	Li Dapeng et al.，2020
RZ29	花岗闪长质片麻岩	栾家界	LA-ICP-MS	3069	17	Liu Shuwen et al.，2017
19LJ01-4	闪长片麻岩	栾家界	LA-ICP-MS	3018	42	Liu Jin et. al.. 2022
19LJ01-7	闪长片麻岩	栾家界	LA-ICP-MS	3078	44	Liu Jin et. al.. 2022
19LJ02-4	闪长片麻岩	栾家界	LA-ICP-MS	3062	59	Liu Jin et. al.. 2022
19LJ01-11	花岗闪长质片麻岩	栾家界	LA-ICP-MS	3093	54	Liu Jin et. al.. 2022
19LJ03-6	花岗闪长质片麻岩	栾家界	LA-ICP-MS	3076	22	Liu Jin et. al.. 2022
塔里木						
19AKZ09，Akazi	奥长花岗质片麻岩	塔里木西南	LA-ICP-MS	3185	11	Ge Rongfeng et al.，2022
20AKZ19，Akazi	英云闪长片麻岩	塔里木西南	LA-ICP-MS	3154	26	Ge Rongfeng et al.，2022
19AKZ04，Akazi	英云闪长片麻岩	塔里木西南	LA-ICP-MS	3060	15	Ge Rongfeng et al.，2022
1011AK-PVI-ZS2	铁镁质麻粒岩	塔里木西南	LA-ICP-MS	3137	4	郭新成等,2013
扬子板块						
LH12	花岗片麻岩	撮科杂岩	LA-ICP MS	3061	23	Cui Xiaozhuang et al.，2021
LH14	花岗片麻岩	撮科杂岩	LA-ICP MS	3074	16	Cui Xiaozhuang et al.，2021
LH15	花岗片麻岩	撮科杂岩	SHRIMP	3110	6	Cui Xiaozhuang et al.，2021

样品号	岩性	采样地点	分析方法	原岩年龄（Ma）	±1σ	资料来源
			印度			
AKS242B	花岗闪长岩	Kolichal	SHRIMP	3152	6	Yang Chengxue et al., 2023
DJ7B	花岗岩	Otayanchal	SHRIMP	3155	12	Yang Chengxue et al., 2023
DJ22	花岗闪长岩	Kappalli	SHRIMP	3163	10	Yang Chengxue et al., 2023
DJ148	花岗岩	Kundupalli	SHRIMP	3152	12	Yang Chengxue et al., 2023
DJ159	辉长闪长岩	Konnakadu	SHRIMP	3156	13	Yang Chengxue et al., 2023
DJ234	花岗岩	Vellad	SHRIMP	3146	14	Yang Chengxue et al., 2023
18ID168	花岗片麻岩	Nelligere	LA-ICP MS	3023	22	Ao Wenhao et al., 2021
18ID356	花岗片麻岩	Kibbanahalli	LA-ICP MS	3158	8.6	Ao Wenhao et al., 2021
BL7	花岗片麻岩	BGC	LA-ICP MS	3115	10	Chakraborti et al., 2019
73	辉长斜长岩	Coorg Block	LA-ICP MS	3176	7	Anoop et al., 2021
77	辉长斜长岩	Coorg Block	LA-ICP MS	3174	8	Anoop et al., 2021
95c	辉长斜长岩	Coorg Block	LA-ICP MS	3143	12	Anoop et al., 2021
97b	紫苏花岗岩	Coorg Block	LA-ICP MS	3110	24	Anoop et al., 2021
APK-1	麻粒岩	Coorg Block	LA-ICP MS	3090	12	Yu Bing et al., 2022
KPT	麻粒岩	Coorg Block	LA-ICP MS	3110	22	Yu Bing et al., 2022
KPK	麻粒岩	Coorg Block	LA-ICP MS	3021	16	Yu Bing et al., 2022
RPM	麻粒岩	Coorg Block	LA-ICP MS	3090	12	Yu Bing et al., 2022
EPA	麻粒岩	Coorg Block	LA-ICP MS	3176	27	Yu Bing et al., 2022
AKS245	辉长岩	Kolichal	SHRIMP	3167	17	Yang Chengxue et al., 2023
AKS276B	辉长岩	Kolichal	SHRIMP	3115	14	Yang Chengxue et al., 2023
DJ255	辉长岩	Kolichal	SHRIMP	3144	14	Yang Chengxue et al., 2023
DJ30	辉长岩	Kolichal	SHRIMP	3141	16	Yang Chengxue et al., 2023
DJ81	辉长岩	Kolichal	SHRIMP	3140	10	Yang Chengxue et al., 2023
DJ160	辉长岩	Kolichal	SHRIMP	3137	7	Yang Chengxue et al., 2023
DJ75	角闪岩	Coorg	LA-ICP MS	3147	9	Yang Chengxue et al., 2023
DJ157	褐煤	Coorg	LA-ICP MS	3094	8	Yang Chengxue et al., 2023
DJ167	褐煤	Coorg	LA-ICP MS	3077	9	Yang Chengxue et al., 2023
BR-5	片麻岩	BR Hill	LA-ICP MS	3100	26	Ratheesh-Kumar et al., 2016
CA33PB	石英岩	Bastar 克拉通	Sm-Nd 定年	3005	14	Nandi et al., 2023
Hassan Gneiss	TTG	达瓦克拉通	Rb-Sr	3162	61	Monrad ,1983
Holenarsipur gneiss	TTG	达瓦克拉通	Rb-Sr	3020	125	Bhaskar Rao et al., 1983
Halekote Gneiss	TTG	达瓦克拉通	U-Pb	3106	32	Sarma et al., 2012
Chitradurga gneiss	TTG	达瓦克拉通	Pb-Pb	3028	28	Taylor et al., 1984
Chitradurga granite	TTG	达瓦克拉通	Rb-Sr	3080	110	Taylor et al., 1984
Chitradurga granite	TTG	达瓦克拉通	Rb-Sr	3175	45	Taylor et al., 1984
Chitradurga gneisses	TTG	达瓦克拉通	Rb-Sr	3060	160	Taylor et al., 1984
Chitradurga gneisses	TTG	达瓦克拉通	Rb-Sr	3190	100	Taylor et al., 1984
Chitradurga granite	TTG	达瓦克拉通	Rb-Sr	3030	110	Taylor et al., 1984
Chitradurga gneiss	TTG	达瓦克拉通	Rb-Sr	3150		Taylor et al., 1984
Arsilkere tank	TTG	达瓦克拉通	Pb-Pb	3184	26	Maibam et al., 2011
Tagadur WD4	TTG	达瓦克拉通	Pb-Pb	3119	19	Maibam et al., 2011
Tagadur WD5	TTG	达瓦克拉通	Pb-Pb	3055	22	Maibam et al., 2011
Kodihalli Granitic gneiss	TTG	达瓦克拉通	Pb-Pb	3156	9	Maibam et al., 2011
Kaladurga Gneissic clast	TTG	达瓦克拉通	Pb-Pb	3190	26	Maibam et al., 2011
Gray granite	TTG	达瓦克拉通	SHRIMP	3146	26	Jayananda et al., 2015
Eastern leucocratic gneiss	TTG	达瓦克拉通	SHRIMP	3100	4	Jayananda et al., 2015
chikmagalur granite	TTG	达瓦克拉通	SHRIMP	3153	4	Jayananda et al., 2015
RAG1	花岗岩	辛格布姆	Sm-Nd 定年	3050	0	Upadhyay et al., 2019
RAG2	花岗岩	辛格布姆	Sm-Nd 定年	3050	0	Upadhyay et al., 2019
RAG6	花岗岩	辛格布姆	Sm-Nd 定年	3050	0	Upadhyay et al., 2019
JAS41	花岗岩	辛格布姆	Sm-Nd 定年	3050	0	Upadhyay et al., 2019
BLR184	角砾岩	辛格布姆	SHRIMP	3123	7	Augé et al., 2003

样品号	岩性	采样地点	分析方法	原岩年龄(Ma)	±1σ	资料来源
BLR187	角砾岩	辛格布姆	SHRIMP	3119	6	Augé et al., 2003
BLR191	辉长岩	辛格布姆	SHRIMP	3122	5	Augé et al., 2003
sc07/1	花岗岩	辛格布姆	LA-ICP MS	3087	3	Nelson et al., 2014
BG64	花岗岩	辛格布姆	LA-ICP MS	3080	8	Mishra et al., 1999
BE154	花岗岩	辛格布姆	LA-ICP MS	3092	5	Mishra et al., 1999
JA1	花岗岩	辛格布姆	LA-ICP MS	3099	14	Manikyamba et al., 2020
wds-32	花岗闪长岩	达瓦克拉通	LA-ICP MS	3141	10	Ranjan et al., 2020
wds-24	奥长花岗岩	达瓦克拉通	LA-ICP MS	3154	21	Ranjan et al., 2020
JD-2	TTG	达瓦克拉通	SHRIMP	3154	45	Rekha et al., 2013
ZEN-8	TTG	达瓦克拉通	SHRIMP	3131	28	Rekha et al., 2013
ZEN-31	TTG	达瓦克拉通	SHRIMP	3128	60	Rekha et al., 2013
GHH-22.4	英云闪长岩	达瓦克拉通	LA-ICP MS	3197	11	Ravindran et al., 2023
CHK-36	花岗岩	达瓦克拉通	LA-ICP MS	3049	21	Ravindran et al., 2023
SG-29.1	奥长花岗岩	达瓦克拉通	LA-ICP MS	3178	10	Ravindran et al., 2023
GHH-22.1	英云闪长岩	达瓦克拉通	LA-ICP MS	3026	26	Ravindran et al., 2023
CHH-22.3	英云闪长岩	达瓦克拉通	LA-ICP MS	3010	25	Ravindran et al., 2023
SG-32.1	奥长花岗岩	达瓦克拉通	LA-ICP MS	3160	12	Ravindran et al., 2023
SG-32.2	奥长花岗岩	达瓦克拉通	LA-ICP MS	3163	10	Ravindran et al., 2023
SG-43.1	奥长花岗岩	达瓦克拉通	LA-ICP MS	3107	20	Ravindran et al., 2023
DHR07	超基性岩	Nuggihalli greenstone belt	Sm-Nd 测年	3125	120	Mukherjee et al., 2012
WD-2	石英绿泥石片岩	达瓦克拉通	LA-ICP MS	3160	34	Maibam et al., 2011
WD-4	TTG	达瓦克拉通	LA-ICP MS	3091	8	Maibam et al., 2011
WD-5	TTG	达瓦克拉通	LA-ICP MS	3060	8	Maibam et al., 2011
WD-6	花岗片麻岩	达瓦克拉通	LA-ICP MS	3067	9	Maibam et al., 2011
WD-7	片麻岩	达瓦克拉通	LA-ICP MS	3183	9	Maibam et al., 2011
18DC12	奥长花岗质片麻岩	达瓦克拉通	SHRIMP	3178	10	Guitreau et al., 2017
B1	科马提岩	达瓦克拉通	Sm-Nd 测年	3137	19	Maya et al., 2017
Ind55C	花岗岩	达瓦克拉通	SHRIMP	3134	4	Jayananda et al., 2015
CUN1A	片麻岩	达瓦克拉通	SHRIMP	3103	15	Jayananda et al., 2015
HL5A	奥长花岗岩	达瓦克拉通	SHRIMP	3106	17	Jayananda et al., 2015
Ind55B	奥长花岗岩	达瓦克拉通	SHRIMP	3087	11	Jayananda et al., 2015
HL1A	奥长花岗岩	达瓦克拉通	SHRIMP	3100	13	Jayananda et al., 2015
PG-2	TTG	达瓦克拉通	Pb-Pb	3127	8	Jayananda et al., 2020
HNP-10	石英片岩	达瓦克拉通	SHRIMP	3105	10	Dasgupta et al., 2019
WY-7	石英片岩	Coorg Block	LA-ICP MS	3010	30	Yang Qiongyan et al., 2016
WY-8	石英片岩	Coorg Block	LA-ICP MS	3168	47	Yang Qiongyan et al., 2016
WY-10	花岗岩	Coorg Block	LA-ICP MS	3162	28	Yang Qiongyan et al., 2016
WY-15	橄榄岩	Coorg Block	LA-ICP MS	3199	26	Yang Qiongyan et al., 2016
NDK-1	花岗岩	Coorg Block	LA-ICP MS	3172	6	Santosh et al., 2016
NDV-1	石英云母片岩	Coorg Block	LA-ICP MS	3120	7	Santosh et al., 2016
NDV-2	石英云母片岩	Coorg Block	LA-ICP MS	3146	12	Santosh et al., 2016
BTD-1	花岗岩	Coorg Block	LA-ICP MS	3140	6	Santosh et al., 2015
CHTD-1	花岗岩	Coorg Block	LA-ICP MS	3184	5	Santosh et al., 2015
KIN1D	花岗岩	Coorg Block	LA-ICP MS	3163	6	Santosh et al., 2015
KUT2D	花岗岩	Coorg Block	LA-ICP MS	3133	12	Santosh et al., 2015
KUT3DA	闪长岩	Coorg Block	LA-ICP MS	3158	8	Santosh et al., 2015
KUT3DB	闪长岩	Coorg Block	LA-ICP MS	3156	10	Santosh et al., 2015
PBTD-1	花岗岩	Coorg Block	LA-ICP MS	3153	9	Santosh et al., 2015
PDRD-1	花岗岩	Coorg Block	LA-ICP MS	3172	6	Santosh et al., 2015
TKLD-1	凝灰岩	Coorg Block	LA-ICP MS	3173	16	Santosh et al., 2015
ARJ	花岗岩	Coorg Block	LA-ICP MS	3168	28	Amaldev et al., 2016
SDP	变质泥岩	Coorg Block	LA-ICP MS	3049	32	Amaldev et al., 2016
PDY	镁质砾岩	Coorg Block	LA-ICP MS	3182	20	Amaldev et al., 2016

样品号	岩性	采样地点	分析方法	原岩年龄(Ma)	±1σ	资料来源
MDU	黑云母片麻岩	Coorg Block	LA-ICP MS	3135	14	Amaldev et al., 2016
CB11C	白云母片岩	BC	LA-ICP MS	3127	6	Nandi et al., 2023
澳大利亚						
2008371067	花岗岩	south of Iron Knob	SHRIMP	3149	3	Fraser et al. . 2010
2008371080	花岗岩	south of Iron Knob	SHRIMP	3158	2	Fraser et al. . 2010
2008371086	花岗岩	south of Iron Knob	SHRIMP	3155	4	Fraser et al. . 2010
2008371087	花岗岩	south of Iron Knob	SHRIMP	3152	19	Fraser et al. . 2010
2008371085	花岗片麻岩	west of Iron Knob	SHRIMP	3151	3	Fraser et al. . 2010
178185	粗粒辉长岩	Soanesville greenstone belt	SHRIMP II	3182	2	Kranendonk et al., 2010
160957	火山碎屑岩	东斯特雷利绿岩带	SHRIMP II	3192	7	Kranendonk et al., 2010
180039	长英质凝灰岩	绿岩带基地	SHRIMP II	3180	6	Kranendonk et al., 2010
180098	流纹凝灰岩	Pilbara Well greenstone belt	SHRIMP II	3176	3	Kranendonk et al., 2010
178045	中粒石英岩	Cheearra greenstone belt	SHRIMP II	3162	28	Kranendonk et al., 2010
南非						
MS6	片麻岩	Leo Man Shield	SHRIMP	3061	5	Waele et al., 2015
MS7	花岗岩	Leo Man Shield	SHRIMP	3107	32	Waele et al., 2015
MS8	石英岩	Leo Man Shield	SHRIMP	3094	16	Waele et al., 2015
G1526	片麻岩	Kenema Assemblage	SHRIMP	3169	12	Waele et al., 2015
588b	英云闪长岩	Mesoarchaean	SHRIMP	3122	11	Westraat et al., 2005
586	花岗岩	Mesoarchaean	SHRIMP	3113	3	Westraat et al., 2005
Kub23	片麻岩	卡普瓦尔	LA-ICP MS	3160	11	Taylor et al., 2012
Kub17	片麻岩	卡普瓦尔	LA-ICP MS	3161	15	Taylor et al., 2012
Kub14	片麻岩	卡普瓦尔	LA-ICP MS	3083	9	Taylor et al., 2012
Lu9	片麻岩	卡普瓦尔	LA-ICP MS	3114	10	Taylor et al., 2012
Z3	英云闪长岩	卡普瓦尔	SHRIMP	3034	2	Moser et al. ,2001
Z5	英云闪长岩	卡普瓦尔	SHRIMP	3032	3	Moser et al. ,2001
Z8	英云闪长岩	卡普瓦尔	SHRIMP	3070	2	Moser et al. ,2001
Z3	英云闪长片麻岩	卡普瓦尔	SHRIMP	3016	2	Moser et al. ,2001
Z2	花岗岩	卡普瓦尔	SHRIMP	3032	8	Moser et al. ,2001
Z4	花岗岩	卡普瓦尔	SHRIMP	3038	2	Moser et al. ,2001
Z5	花岗岩	卡普瓦尔	SHRIMP	3051	3	Moser et al. ,2001
S30Y	片麻岩	刚果	Pb-Pb	3144	3	Tchemeni et al., 2004
TR9237	片麻岩	刚果	Pb-Pb	3088	2	Tchemeni et al., 2004
JA-3	TTG	刚果	LA-ICP MS	3155	11	Akame et al., 2020
DS30509	英云闪长片麻岩	马达加斯加	SHRIMP	3176	6	Schofield et al., 2010
LA-307b	英云闪长片麻岩	马达加斯加	SHRIMP	3187	2	Tucker et al., 1999
MH73	英云闪长片麻岩	马达加斯加	SHRIMP	3154	5	Schofield et al., 2010
BT30192	英云闪长片麻岩	马达加斯加	SHRIMP	3187	15	Schofield et al., 2010
西格陵兰						
306	英云闪长岩	northern Akia Terrane	LA-ICPMS	3019	12	Gardiner et al., 2019
566	英云闪长岩	northern Akia Terrane	LA-ICPMS	3018	13	Gardiner et al., 2019
575	花岗岩	northern Akia Terrane	LA-ICPMS	3013	16	Gardiner et al., 2019
158	英云闪长岩	northern Akia Terrane	LA-ICPMS	3008	9	Gardiner et al., 2019
325	英云闪长岩	northern Akia Terrane	LA-ICPMS	3002	13	Gardiner et al., 2019
159	英云闪长岩	northern Akia Terrane	LA-ICPMS	3019	11	Gardiner et al., 2019
173	淡色辉长岩	northern Akia Terrane	LA-ICPMS	3007	9	Gardiner et al., 2019
307	英云闪长岩	northern Akia Terrane	LA-ICPMS	3011	10	Gardiner et al., 2019
740	含辉石脉体	west Maniitsoq Island	SHRIMP II	3009	3	Yakymchuk et al., 2020
202	辉石晶斜辉石-斜辉石脉体	west Maniitsoq Island	SHRIMP II	3001	14	Yakymchuk et al., 2020

样品号	岩性	采样地点	分析方法	原岩年龄(Ma)	±1σ	资料来源
524226	正片麻岩	Maniitsoq	离子探针	3035	3	Schersten et al., 2013
524204	斜长片麻岩中的重结晶	Maniitsoq	离子探针	3000	5	Schersten et al., 2013
524216	正片麻岩	Maniitsoq	离子探针	3000	6	Schersten et al., 2013
524217	多云母角砾岩细粒碎屑基质	Maniitsoq	离子探针	3003	5	Schersten et al., 2013
524282	正片麻岩	Maniitsoq	离子探针	3003	6	Schersten et al., 2013
582	正片麻岩	Maniitsoq	SHRIMP II	3014	8	Steenfelt et al., 2020
871	奥长花岗岩	Maniitsoq	SHRIMP II	3008	15	Olierook et al., 2020
873	奥长花岗岩	Maniitsoq	SHRIMP II	3011	6	Olierook et al., 2020
1415	奥长花岗岩	Maniitsoq	SHRIMP II	3013	12	Olierook et al., 2000
289246	正片麻岩	Fiskefjord	SHRIMP	3050	7	Garde et al., 2000
339199	正片麻岩	Fiskefjord	SHRIMP	3035	7	Garde et al., 2000
339223	正片麻岩	Fiskefjord	SHRIMP	3044	7	Garde et al., 2000
477678	英云闪长岩	Qussuk	离子探针	3058	4	Garde et al., 2012
278886	正片麻岩	Iganannguit	SHRIMP II	3008	14	Garde et al., 2000
289177	正片麻岩	Qussuk granite	SHRIMP II	3001	6	Garde et al., 2000
289278	正片麻岩	Nuup Kangerlua	ICPMS	3021	19	Næraa et al., 2012
283347	正片麻岩	Nuup Kangerlua	ICPMS	3038	10	Næraa et al., 2012
477321	正片麻岩	Nuup Kangerlua	SHRIMP II	3040		Hollis et al., 2005
479606	正片麻岩	Nuup Kangerlua	SHRIMP II	3064		Hollis et al., 2005
481201	正片麻岩	Nuup Kangerlua	SHRIMP II	3072		Hollis et al., 2005
481227	正片麻岩	Nuup Kangerlua	SHRIMP II	3046		Hollis et al., 2005
481311	正片麻岩	Nuup Kangerlua	SHRIMP II	3048		Hollis et al., 2005
479060	正片麻岩	Nuup Kangerlua	SHRIMP II	3048		Hollis et al., 2005
479813	正片麻岩	Nuup Kangerlua	SHRIMP II	3050		Hollis et al., 2005
311	正片麻岩	Fiskefjord	SHRIMP II	3006		Hollis et al., 2005
479049	正片麻岩	Nuup Kangerlua	SHRIMP II	3055		Hollis et al., 2005
479665	正片麻岩	Nuup Kangerlua	SHRIMP II	3053		Hollis et al., 2005
216	花岗岩	Finnefjeld	LA-ICPMS	3059	6	Hollis et al., 2005
477320	花岗岩	Qussuk peninsula	离子探针	3005	3	Garde et al., 2007
479827	夹有安山岩变质火山岩的细粒均质片岩	central Bjørneøen	离子探针	3071	1	Garde et al., 2007
540428	片麻岩	Taserssuaq	SHRIMP II	3127	12	Rosing et al., 2001
524204	黑云母片麻岩	Maniitsoq	SHRIMP II	3000	5	Schersten et al., 2013
524216	黑云母闪长岩	Maniitsoq	SHRIMP II	3000	6	Schersten et al., 2013
524217	角砾岩	Maniitsoq	SHRIMP II	3003	5	Schersten et al., 2013
524282	片麻岩	Maniitsoq	SHRIMP II	3003	6	Schersten et al., 2013
565	褐铁矿	norite belt	LA-ICP MS	3025	18	Waterton et al., 2020
585	黑铁矿	norite belt	LA-ICP MS	3003	9	Waterton et al., 2020
875	石英岩	norite belt	LA-ICP MS	3010	4	Waterton et al., 2020
811	粗粒岩	norite belt	LA-ICP MS	3000	4	Waterton et al., 2020
北美洲						
MLR-08	片麻岩	小洛基山	LA-ICP MS	3179	9.9	Gifford et al., 2018
MLR-03	石榴石角闪岩	小洛基山	LA-ICP MS	3007	7	Gifford et al., 2018
03BBL1	花岗岩	黑岩区	SHRIMP	3078	23	Grace et al., 2006
01SWP5	变辉长岩	黑岩区	SHRIMP	3010	1	Grace et al., 2006
03BBL25	花岗岩	黑岩区	Sm-Nd 定年	3100		Grace et al., 2006
MR4-74	英云闪长岩	Madison 山	X 射线	3099	48	Mueller et al., 1993
MR4-75	英云闪长岩	Madison 山	X 射线	3142	21	Mueller et al., 1993
MRV-8A	片麻岩	大瀑布	SHRIMP	3142	2	Bickford et al., 2006
ON200	英云闪长岩	坦尼斯湖		3051	2	Davis et al., 1998
C83-32	英云闪长岩	锡达湖		3172	18	Corfu et al., 1988
49	花岗闪长岩	西苏必利尔省	LA-ICP MS	3132	7	Lankvelt et al., 2016
CB96-73A	花岗闪长岩	阿素湖	LA-ICP MS	3180	6	BöHm et al., 2003

样品号	岩性	采样地点	分析方法	原岩年龄（Ma）	±1σ	资料来源
CB96-42	片麻岩	阿素湖	LA-ICP MS	3191	5	BöHm et al., 2003
CB96-48A	片麻岩	阿素湖	LA-ICP MS	3169	10	BöHm et al., 2003
CB00-56	片麻岩	阿素湖	LA-ICP MS	3165	28	BöHm et al., 2003
98KYT-40	英云闪长岩	Caribou Lake area	Sm-Nd 定年	3075		Tomlinson et al., 2004
98KYT-42	英云闪长岩	Caribou Lake area	Sm-Nd 定年	3075		Tomlinson et al., 2004
95DS-211	英云闪长岩	Marmion east	Sm-Nd 定年	3002		Tomlinson et al., 2004
95DS-24	英云闪长岩	Marmion east	Sm-Nd 定年	3002		Tomlinson et al., 2004
96GRS-4001H	英安岩	Tashota area	Sm-Nd 定年	3056		Tomlinson et al., 2004
			南美洲			
Mi21	片麻岩	乌拉圭	LA-ICP-MS	3137.5	4.4	Henri et al., 2021
Mi30	黑云母片麻岩	乌拉圭	LA-ICP-MS	3074	6.9	Henri et al., 2021
BRJC-16	花岗岩	Gaviao block	TIMS	3146	24	Leal et al., 1998
SSR526A	花岗闪长片麻岩	Gaviao block	TIMS	3040	15	Peucat et al., 2002
MJ316	混合岩	South American Platform	SHRIMP	3055	140	Sato et al., 2003
OPU6433	混合岩	巴西	SHRIMP	3143	13	Medeiros et al., 2017
OPU6432	混合岩	巴西	激光剥蚀	3136	8	Medeiros et al., 2017
OPU6355	混合岩	巴西	激光剥蚀	3097	24	Medeiros et al., 2017
OPU6357	混合岩	巴西	激光剥蚀	3091	24	Medeiros et al., 2017
LL-344B	混合岩	Gaviao block	SHRIMP	3189	44	Lopes et al., 2021
SV2	片麻岩	Sete Voltas	Pb-Pb	3158		Martin et al., 1997
AC-4E	片麻岩	Lagoa do Morro	SHRIMP	3184	6	Nutmanet al., 1993
VZP65	片麻岩	Serra do Eixo Massif	Pb-Pb SHRIMP	3158	5	Santos-Pinto et al., 2012
ARN-60.1/UMB-60.1	花岗岩	Caldeirãozinho Suite	Pb-Pb	3103	4	Santos-Pinto et al., 2012
UMB-164	花岗岩	Caldeirãozinho Suite	Pb-Pb	3130	7	Santos-Pinto et al., 2012
JC-706	二长花岗岩	Serra do Eixo Massif	Pb-Pb	3156	7	Santos-Pinto et al., 2012
PO-9	TTG	Serrinha nucleus		3085		Oliveira et al., 2010
PO-64	TTG	Serrinha nucleus		3085		Oliveira et al., 2010
JUB-21	英云闪长岩	Serrinha nucleus		3120		Oliveira et al., 2010
JM-180B	英云闪长岩	Serrinha nucleus		3120		Oliveira et al., 2010
EO-150A	变质泥岩	Caldeirão Belt	SHRIMP	3152	5	Oliveira et al., 2002
EO-182	镁质花岗岩	Uauá	SHRIMP	3127	14	Oliveira et al., 2019
14EW-20	片麻岩	Uauá	SHRIMP	3125	15	Oliveira et al., 2019
EO178-D	片麻岩	Uauá	LA-ICP MS	3138	20	Oliveira et al., 2019
BACD17-73	英云闪长岩	Bacaba	LA-ICP MS	3001	4	Moreto et al., 2011
BACD9-257	英云闪长岩	Bacaba	LA-ICP MS	3005	9	Moreto et al., 2011
SOS22-107	花岗岩	Sequeirinho orebody	LA-ICP MS	3014	22	Moreto et al., 2015
SOS259-177	花岗岩	Sequeirinho orebody	LA-ICP MS	3010	21	Moreto et al., 2015
SOS39J	角砾岩	Sequeirinho orebody	SHRIMP	3076	5.3	Moreto et al., 2015
OA-46B	花岗岩	Pium Complex	SHRIMP	3002	14	Pidgeon et al., 2000
			欧洲			
A76	英云闪长岩	Iisalmi complex	SIMS	3173	7	Lauri et al., 2011
A937	混合岩	Iisalmi complex	SIMS	3181	6	Lauri et al., 2011
18K	片麻岩	波罗的海地盾	SHRIMP II	3153	5	Sergeev et al., 2007
97A	花岗岩	Vyg 河	SHRIMP	3127	15	Sergeev et al., 2008
42-3	花岗岩	Vyg 河	SHRIMP	3141	27	Sergeev et al., 2008
43-1	花岗岩	Vyg 河	SHRIMP	3146	25	Sergeev et al., 2008
2005	黑云母片麻岩	乌克兰地盾	U—Th—Pb spot	3076	35	Bibikova et al., 2008
2171	黑云母片麻岩	乌克兰地盾	U—Th—Pb spot	3122	16	Bibikova et al., 2008
84-102	黑云母片麻岩	乌克兰地盾	U—Th—Pb spot	3014	22	Bibikova et al., 2008
2197	黑云母片麻岩	乌克兰地盾	U—Th—Pb spot	3024	4	Bibikova et al., 2008
3145/917	火山岩	乌克兰地盾	SHRIMP	3122	9	Savko et al., 2019
26	角闪岩	borehole	LA-ICP MS	3027	10	Lobach-Zhuchenko et al., 2017
25	流纹岩	borehole	LA-ICP MS	3152	10	Lobach-Zhuchenko et al., 2017
65	蛇纹岩	borehole	LA-ICP MS	3130	12	Lobach-Zhuchenko et al., 2017

样品号	岩性	采样地点	分析方法	原岩年龄（Ma）	± 1σ	资料来源
70	花岗闪长岩	borehole	LA-ICP MS	3029	14	Lobach-Zhuchenko et al. , 2017
22	花岗岩	borehole	LA-ICP MS	3073	14	Lobach-Zhuchenko et al. , 2017
南极						
90-121B	片麻岩	Gerard Bluffs	SHRIMP	3060	12	Goodge et al. , 2016
99-301	片麻岩	Gerard Bluffs	SHRIMP	3113	2	Goodge et al. , 2016
9828-101	花岗岩	Mawson Suite	SHRIMP	3194	25	Boger et al. , 2006
9828-039	花岗岩	Mawson Suite	SHRIMP	3174	9	Boger et al. , 2006
9828-190	花岗岩	Mawson Suite	SHRIMP	3160	6	Boger et al. , 2006
9828-210	花岗岩	Mawson Suite	SHRIMP	3162	13	Boger et al. , 2006
33013-8	粗粒片麻岩	Rimmington Bluff	SHRIMP	3180	10	Mikhalsky et al. , 2006
NRL-179	花岗片麻岩	Mawson Suite	SHRIMP	3161	13	Mikhalskyet al. , 2010
48159-4	变辉长岩	Mawson Suite	SHRIMP	3145	12	Mikhalskyet al. , 2010
sPCM-69. 8	微镰石	Mawson Suite	SHRIMP	3181	22	Mikhalskyet al. , 2010